Applied Energy 220 (2018) 545–561

Contents lists available at ScienceDirect

Applied Energy

journal homepage: www.elsevier.com/locate/apenergy

Agrivoltaic systems to optimise land use for electric energy production

Stefano Amaducci[a,*], Xinyou Yin[b], Michele Colauzzi[a]

[a] Department of Sustainable Crop Production, Università Cattolica del Sacro Cuore, via Emilia Parmense, 84, Piacenza, Italy
[b] Centre for Crop Systems Analysis, Department of Plant Sciences, Wageningen University & Research, Droevendaalsesteeg 1, Wageningen, The Netherlands

HIGHLIGHTS

- A simulation platform to simulate crops under agrivoltaic was developed.
- Shading under agrivoltaic improves soil water balance and increases water saving.
- Agrivoltaic conditions increased and stabilized yield of rainfed maize.
- Agrivoltaic doubled renewable energy land productivity.

ARTICLE INFO

Keywords:
Agrivoltaic
Modeling
Land use efficiency
Photovoltaic panels
Maize
Biogas

ABSTRACT

A system combining soil grown crops with photovoltaic panels (PV) installed several meters above the ground is referred to as agrivoltaic systems. In this work a patented agrivoltaic solar tracking system named Agrovoltaico®, was examined in combination with a maize crop in a simulation study. To this purpose a software platform was developed coupling a radiation and shading model to the generic crop growth simulator GECROS. The simulation was conducted using a 40-year climate dataset from a location in North Italy, rainfed maize and different Agrovoltaico configurations (that differ according to panel density and sun-tracking set up). Control simulations for an irrigated maize crop under full light were added to results.

Reduction of global radiation under the Agrovoltaico system was more affected by panel density (29.5% and 13.4% respectively for double density and single density), than by panel management (23.2% and 20.0% for sun-track and static panels, respectively).

Radiation reduction, under Agrovoltaico, affected mean soil temperature, evapotranspiration and soil water balance, on average providing more favorable conditions for plant growth than in full light. As a consequence, in rainfed conditions, average grain yield was higher and more stable under agrivoltaic than under full light. The advantage of growing maize in the shade of Agrovoltaico increased proportionally to drought stress, which indicates that agrivoltaic systems could increase crop resilience to climate change.

The benefit of producing renewable energy with Agrovoltaico was assessed using the Land Equivalent Ratio, comparing the electric energy produced by Agrovoltaico cultivated with biogas maize to that produced by a combination of conventional ground mounted PV systems and biogas maize in monoculture. Land Equivalent Ratio was always above 1, it increased with panel density and it was higher with sun tracking than with static panels. The best Agrivoltaico scenario produced twice as much energy, per unit area, as the combination of ground mounted PV systems and biogas maize in monoculture. For this Agrivoltaico can be considered a valuable system to produce renewable energy on farm without negatively affecting land productivity.

1. Introduction

Worldwide energy demand is expanding due to an increasing global population and energy use by industry. At the same time, the threat of global warming is reshaping strategies of energy production; the EU decreed that by 2020, 20% of the energy must come from renewable sources, (Renewable Energy Directive, 2009/28/EC), which should become at least 27% by 2030 (EC COM(2016) 767 final/2). Despite its intimate connection with sustainable development [1], renewable energy production is not immune to criticism, especially when it interferes with actual land use, as demonstrated by the fuel vs food debate [2].

Among renewable energies, solar photovoltaics (PV) is the fastest growing power generating technology [3]. A number of studies have addressed the potential impacts of PV plants, particularly in terms of

* Corresponding author.
E-mail address: stefano.amaducci@unicatt.it (S. Amaducci).

https://doi.org/10.1016/j.apenergy.2018.03.081
Received 10 January 2018; Received in revised form 28 February 2018; Accepted 25 March 2018
Available online 31 March 2018

the conflict that large scale PV plants can generate on agricultural land [4–7] while Calvert and Mabee [8] developed a methodology to compare the production potential and land-use efficiency of PV and bioenergy solutions. Although PV energy has a low land requirement compared to other renewable-energy options [9], its landscape integration should be designed to minimize adverse land use changes and favor community acceptance [10]. Combination of PV power production and agricultural activities has many potential declinations [11]. While integration of PV panels to agricultural infrastructures, to drying systems [12] or its use for waste water purification [13] and water pumping [14] proved to be technically feasible and provides multiple benefits [11], the use of agricultural land to install ground mounted PV has been constrained by governments and local authorities to avoid soil consumption, landscape impact, and competition with food production [15]. To date, PV systems designed to combine PV energy production with food crops in the same installation are mainly related to greenhouse applications, as an energy saving strategy [16] or to increase farmer's income [17]. Photovoltaic greenhouses are widespread in southern Europe, [18] and have seen a rapid expansion in China [19] thanks to incentive tariffs. In contrast, few PV systems have been designed to overcome the energy vs food competition by combining PV energy production with crops in open field conditions, a concept that was first proposed by Goetzberger and Zastrow [20]. An experimental system combining static PV panels installed 4 m above the ground, with soil grown crops under the panels (as described in [21;22]), was referred to as an *agrivoltaic system*. Such systems are based on the concept that a partial shading can be tolerated by crops and it might reduce water consumption by evapotranspiration during the summer and under drought conditions [23]. It has even been shown that a shade tolerant crop, such as lettuce, grown under PV panels adapts its morphology (e.g. producing wider leaves) without yield reduction, and that overall electricity coupled to lettuce production under agrivoltaic generated a 30% increase in economic value compared to conventional agriculture.

It was proposed that advantages of agrivoltaic systems might be related to their similarity to agroforestry systems [24]; the PV panels protect crops from excessive heat and provide soil temperature mitigation [25], which could imply that agrivoltaic systems are more resilient to climate change than monocultures [24]. Dinesh and Pearce [23] performed a modelling analysis in which lettuce cultivation under PV panels was also simulated in terms of crop yield and energy gain. They showed that the value of solar generated electricity coupled to shade tolerant crop production created an over 30% increase in economic value in farms deploying agrivoltaic systems.

In a recent paper, Majudmar and Pasqualetti [26] propose the implementation of agrivoltaic systems as a sustainable strategy in peri-urban areas to generate carbon-free electricity and preserve the agricultural land by providing urban growth boundaries and increasing land value and farmers' benefits. The successful implementation of agrivoltaic systems ultimately depends on farmers' acceptance, which is based on their perception of the benefits of agrivoltaic systems. Increased land value [23] and land productivity [21] are very convincing attributes of agrivoltaic systems and utility companies could further stimulate development of agrivoltaics with incentives for farmers [26]. An understanding that crop yield under agrivoltaics is not seriously affected (or in some cases remains equal or is increased) and/or water use efficiency can increase [23] would provide a further push towards the diffusion of agrivoltaic systems in open fields. The additional energy production would not radically transform farmers' businesses, but it would complement their income, increase self-consumption and ultimately reduce public spending on renewable energy [17].

Modelling analyses have shown that production in an agrivoltaic system can be optimized by modifying the architecture of the panels [23,27] and crop productivity can be stimulated by adjusting the tilting of the panel during the cropping cycle [27]. A step forward would therefore be to install PV panels that can move in order to either maximize energy production or food production, or to optimize both [27]. Early research on agrovoltaics was limited to case studies with fixed panels [22] and only one very recent research reports on mobile 1-axis PV system [27]. The system Agrovoltaico® (hereafter referred to as *Agrovoltaico*) was designed and built on a large scale to combine the cultivation of field crops, such as maize (*Zea mays* L.) and winter wheat (*Triticum aestivum* L.), with the production of solar energy on the same land unit. The first two *Agrovoltaico* systems were installed in 2012 in Castelvetro Piacentino [28] and Monticelli d'Ongina [29] (Po valley, Northern Italy, N 45.09° E 10.00° and N 45.07° E 9.93°, respectively) covering an area of 7 ha and 20 ha, respectively.

Considering that radiation in agrivoltaic systems is reduced due to partial shading and many economically important field crops such as maize are considered not shade-tolerant, we developed a modeling platform that not only simulates maize production under a specific agrivoltaic system, but also optimizes crop yield and energy production by adjusting the agrivoltaic system configuration. The principal aims of this study were two-fold. The first was to simulate the production of maize cultivated under the partial shading of the *Agrovoltaico* system using a bespoke radiation model and the GECROS crop model [30]. The second was to compare both energy and crop production under different configurations of the *Agrovoltaico* system. In particular, four different configurations of the system were compared: static PV panels (F) versus sun tracking PV panels (ST), with each having two different PV panel densities (m^2 PV panel/m^2 ground).

In order to demonstrate the potential of our simulation platform to predict energy production and crop yield under different configurations, and to compare strategies for renewable energy production at farm level, the data produced in this study will be used to compare the global land productivity of *Agrovoltaico* systems to the more common options of either cultivating maize for biogas or producing electrical energy from ground mounted PV systems.

2. Materials and methods

2.1. The Agrovoltaico system

The *Agrovoltaico* system (Fig. 1) is a solar tracking system, built on suspended structures (stilts). On the stilts are mounted horizontal main axis, on which secondary axis holding the solar panels are hinged. The two axes can rotate as they are driven by electric motors interconnected through an innovative control system and wireless communication. Under *Agrovoltaico,* in contrast to traditional ground PV installations, agricultural practices can be performed with standard machinery. One relevant feature of *Agrivoltaico* is that panels are not evenly distributed on the soil surface, and this affects the shading patterns at soil level, with the creation of a band along the main axis of the panel arrays where shade is more intense and another band where the shade only occurs at certain periods during the day.

2.2. Software platform and data

To simulate the growth and production of crops cultivated under the shade of a *Agrovoltaico* system, a software platform was developed in Scilab [31] coupling a radiation and shading model to the generic crop growth simulator GECROS [30]. Scilab is a programming language associated with a rich collection of numerical algorithms covering many aspects of scientific computing problems. The platform is designed to maintain and handle large climatic dataset and different environmental situations using free software relational database (MySQL). The database includes soil information (Regional environmental services) and meteorological series provided by Meteorological Regional Services since 1990. Older meteorological series were reconstructed with the data obtained from the Joint Research Centre (Interpolated AGRI4CAST Meteorological, link; http://agri4cast.jrc.ec.europa.eu/DataPortal/Index.aspx).

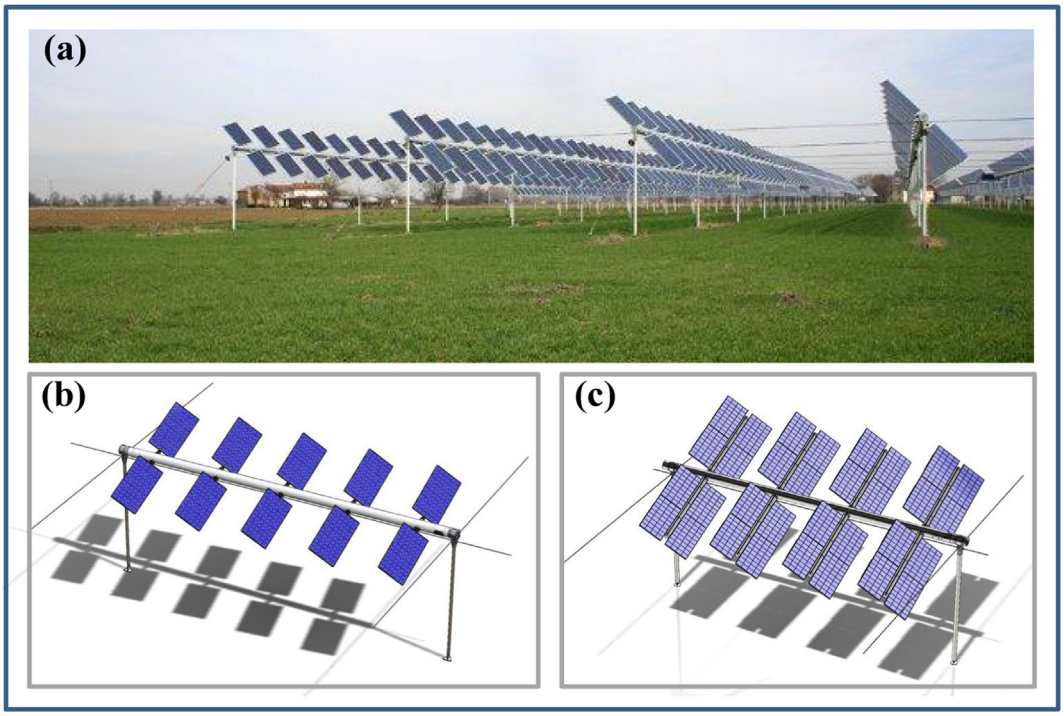

Fig. 1. (a) View of an Agrovoltaico® plant equipped with a dual-axis, sun-track system, (b) stilt unit (release 1) equipped with 5 secondary axis and 10 solar panels, (c) Stilt unit (release 2) equipped with 4 secondary axis and 32 solar panels.

Data of global radiation (kJ m^{-2}) include daily values until 2010 and hourly values thereafter. For the years with missing hourly values, daily global radiation was disaggregated at the needed time step t_s following the procedure described by Collares-Pereira [32] as reported by Wanxiang et al. [33]. Diffuse and direct radiation (R_d and R_b, kJ m^{-2}) were calculated with the model described by Collares-Pereira [32] and implemented according to Al-Rawahi [34]. The hourly dataset for all the other meteorological data (temperature, partial vapour pressure and wind speed) required to feed the subroutines of photosynthesis and evapotranspiration in GECROS were obtained by disaggregation of daily values according to Ephrath et al. [35].

2.3. Shading and radiation model

The model computes direct and diffuse radiation at ground level with a time step $t_s = 0.5$ h and a spatial resolution of 0.12 m. These were chosen to reach the best compromise between computing time and resolution in time and space.

A procedure to compute whether a specific soil portion (square pixel with user defined size) is shaded or receives direct radiation, was developed. These calculations were done as if the solar panel arrays were infinite (or distributed on a very large surface). This implies that whenever the panels project a shadow on the ground, the system takes it into account. For a given geo-localization (latitude and longitude) and day of the year, the procedure computes, at each time step, the sun position [36] and provides sun azimuth γ_s, elevation α_s, (Fig. 4) sunrise s_r (h) and sunset s_s. (h) For the sun-track system, rotation angles of plant axis (main axis, angle θ and secondary axis angle ϕ) were computed with the same time step. Rotation angles (Fig. 2) are computed with:

$$\begin{cases} \tan\theta' = -\frac{\tan\alpha_s}{\cos(\gamma_s+\psi)} \\ \cos\phi = a\cos[\cos\alpha_s \sin(\gamma_s+\psi)] - \frac{\pi}{2} \\ \theta = \begin{cases} \pi + \theta' & \text{if } \theta' < 0 \\ \theta' & \text{if } \theta' > 0 \end{cases} \end{cases} \quad (1)$$

where ψ is the plant layout angle (direction of the main axis) measured from the West - East, positive counter clock. For simulations with static panels (Table 1) angles θ and ϕ were set at 30° and 0°, respectively.

Coordinates were represented within a vectorial based system (Σ) with the basis vector oriented to the North, East and Zenit (NEZ) according to Quaschning and Hanitsch [37].

$$\sum = \{0,N,E,Z\}.$$

The vector **s** (Fig. 5) pointing the sun can be given by:

$$s = \begin{Bmatrix} \cos\gamma_s \cdot \cos\alpha_s \\ \sin\gamma_s \cdot \cos\alpha_s \\ \sin\alpha_s \end{Bmatrix} \quad (2)$$

In the software, solar panels were represented by a single rectangle filled by a grid of dots distributed at user defined density. For simplicity the panel was modelled as a 2D structure, without depth, and mathematically represented as a matrix of coordinates. In our simulations a density of 20 dots per 1 m (400 dots m^{-2}) was adopted. All dots were given by a matrix $\boldsymbol{v}$ in the NEZ-coordinates system.

New $\boldsymbol{v_r}$ coordinates, after axes rotation, were computed for a single grid matrix representing one panel. This step was carried out with the Scilab toolbox CelesteLab [38].

Shading occurs if an object is placed within the position of the sun and the soil surface. The shadow position of a single point $\boldsymbol{p_0} \in \boldsymbol{v_r}$ was determined with the calculation of the position of the point of intersection $\boldsymbol{p_s}$ with the ground in the opposite direction of the vector $\boldsymbol{s}$. The floor (or any shaded surface) was described by a polygon with 4 vectors $\boldsymbol{p_1 \ldots p_4}$, and the vector $\boldsymbol{p_s}$ for the intersection between the straight in sun direction and shaded surface was obtained with the equation:

$$p_s = p_0 - \frac{a \cdot (p_0 - p_1)}{a \cdot s} \quad (3)$$

The vector $\boldsymbol{a}$ is perpendicular to the soil ground (vectors $\boldsymbol{p_1 \ldots p_4}$ or shaded polygon) and is computed with:

$$a = (p_2 - p_1) \times (p_4 - p_1) \quad (4)$$

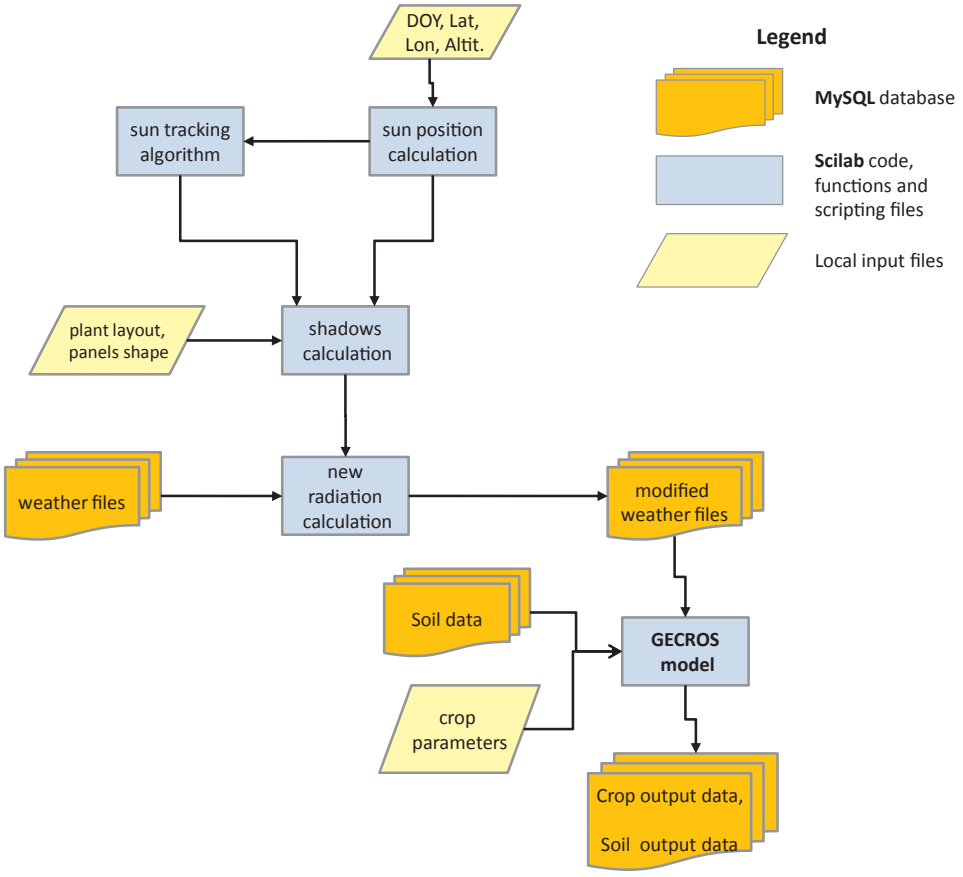

Fig. 2. Diagram of the most relevant elements of the software platform. Data flow is driven by SciLab scripting (db-queries and file inter-change).

In the simulations the polygon $\boldsymbol{p_1 \ldots p_4}$ is a quadrate of size 12 m, which is the distance between the vertical poles supporting the *Agrovoltaico* module. In this work, this polygon represents the 'study area unit' which is centered below the main rotation axis, between two vertical poles (Fig. 5b).

The polygon was divided into $\boldsymbol{n_{pix}} = 10^4$ pixels (0.12 m size) and, at each time step, the state of a pixel (shaded or not-shaded) was determined by overlapping the area of the shade to the study area. The area of the shade was reconstructed at ground level with the projected grid. The information on shadowing has an intrinsic Boolean feature (shaded = 0, non-shaded = 1) which was exploited for efficient data handling and computation. The shaded state of a soil pixel was attributed with the presence of at least 3 shading $\boldsymbol{p_s}$ points within its square polygon and a Boolean matrix ***Sh*** was obtained.

To store the data, a tri-dimensional annual matrix ***Ms.*** was built:

$$Ms(\boldsymbol{p}_{1\ldots npIX}, \boldsymbol{t_n}_{1\ldots nt}, \boldsymbol{t_{DOY}}_{1\ldots 366}) = \begin{pmatrix} m_{1,1} & \cdots & m_{1,nt} \\ \vdots & \ddots & \vdots \\ m_{npix,1} & \cdots & m_{npix,nt} \end{pmatrix}_{DOY=1} \ldots \begin{pmatrix} m_{1,1} & \cdots & m_{1,nt} \\ \vdots & \ddots & \vdots \\ m_{npix,1} & \cdots & m_{npix,nt} \end{pmatrix}_{DOY=366} \quad (5)$$

The dimension along $\boldsymbol{p}$ contains spatial information: the $\boldsymbol{n_{pix}}$ values of the square Boolean $\boldsymbol{S_h}$ matrix, were vectorized in a matrix of size $\boldsymbol{n_{PIX}} \times 1$ and filled at each time step $\boldsymbol{t_n}$. The repetition $\boldsymbol{n_t}$ times of the vectorization at day $\boldsymbol{t_{DOY}}$ occupied the second dimension of matrix ***Ms***. The third dimension is given by the days of a year.

Considering that shaded or non-shaded pixels receive respectively only diffuse or diffuse + direct radiation, matrix ***Ms.*** was used to compute the global radiation column of the input weather file for the ***n***-pixel with:

Table 1
Agrivoltaic arrangements and most relevant geometrical features of the simulated ystems.

Configuration	Code	Sun track	Field layout (ψ)	Tilt angle (degrees)		N panels/ secondary mobile axis	N sec. axis between the stilts	Distance between the stilts (m)	Panels size		Ratio: total panels surface/soil surface	Height of main rotation axis (m)
				θ	ϕ				Length (m)	Width (m)		
Release 1 - sun track	**ST1**	Yes	0°	*Variable*	*Variable*	2	5	12	1.958	0.992	0.13	4.83
Release 1 - static	**F1**	No	0°	30°	0°	2	5	12	1.958	0.992	0.13	4.83
Release 2 - sun track	**ST2**	Yes	0°	*Variable*	*Variable*	8	4	12	1.648	0.992	0.36	4.83
Release 2 - static	**F2**	No	0°	*30°*	*0°*	8	4	12	1.648	0.992	0.36	4.83
Full light	**FL**	–	–	–	–	–	–	–	–	–	–	–

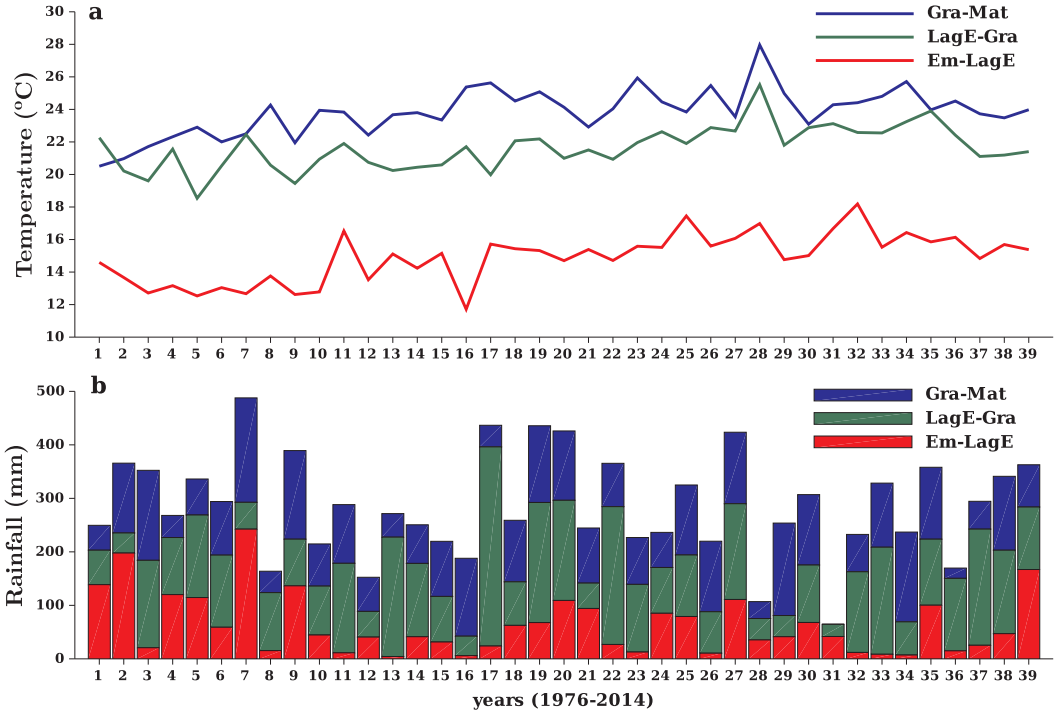

Fig. 3. (a) Air Temperature (°C) and (b) Rainfall (mm) in open air conditions during three periods of simulated crop cycle: seedling mergence-end of lag phase, $DS^{*} \leq 0.15$ (Em-LagE); end lag phase - grain initiation (LagE-Gra); grain initiation - maturity (Gra-Mat).

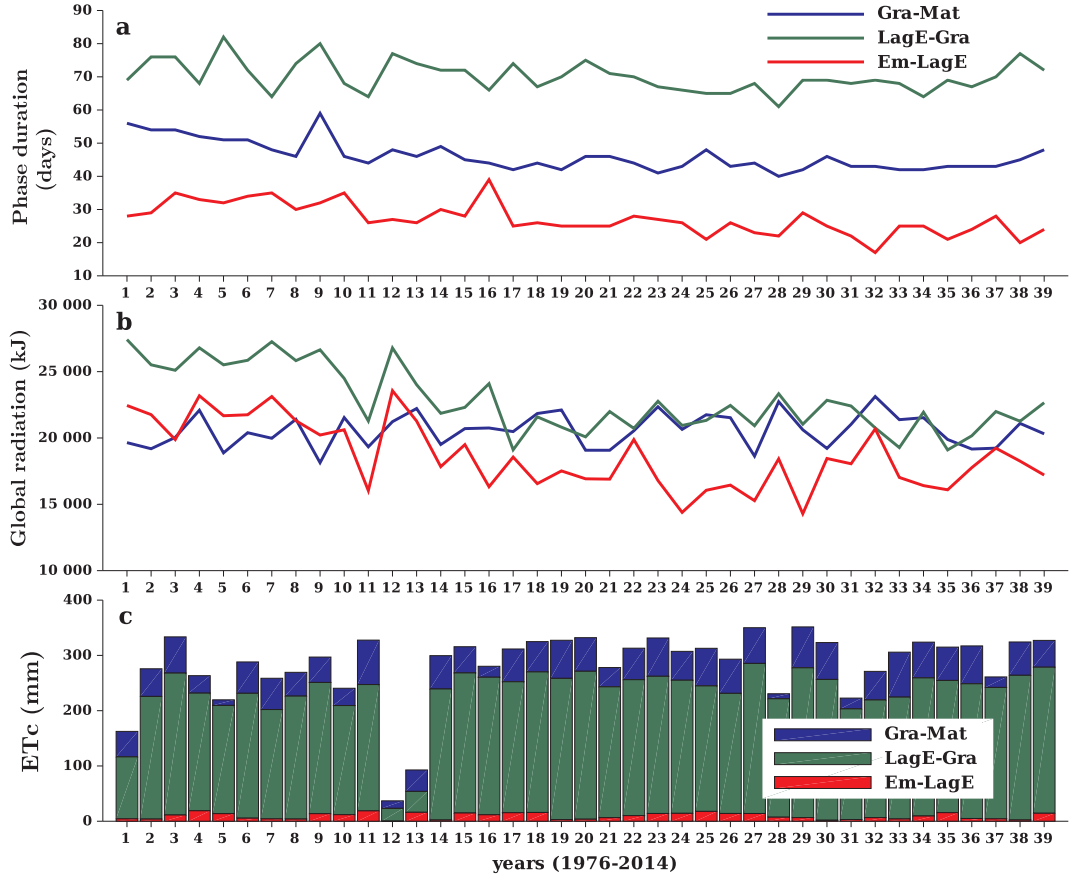

Fig. 4. (a) Phases duration (days) and (b) Global radiation (kJ) and (c) Crop evapotranspirationm, ETc (mm) in open air conditions during three periods of simulated crop cycle: seedling mergence-end of lag phase, $DS^{*} \leq 0.15$ (Em-LagE); end lag phase - grain initiation (LagE-Gra); grain initiation - maturity (Gra-Mat).

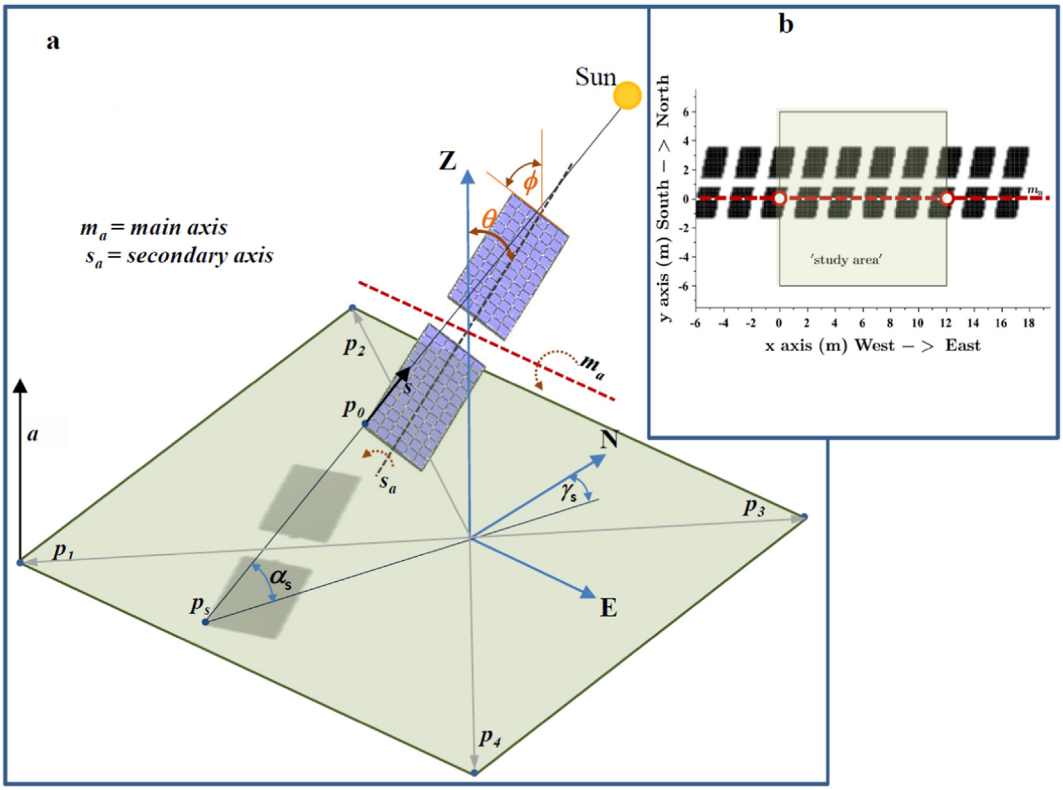

Fig. 5. (a) Reference system and rotation angles of the dual-axis sun track system Agrovoltaico, scenario ST1, see Table 1 for details and geometrical features. (b) Study area unit: shadows to the ground of day 10 June at 16:30 for configuration ST1. The horizontal red line represents the localization of the main rotation axis of the plant and the yellow circles indicate the position of the vertical poles of the Agrovoltaico plant. (For interpretation of the references to colour in this figure legend, the reader is referred to the web version of this article.)

$$(R_g)_{p_n,t_n,DOY} = (R_b \cdot Ms + R_d)_{p_n,t_n,DOY}$$
$$with: \begin{cases} p_n,1...n_{PIX},n_{PIX} = 10^4 \\ t_n,1...n_t,n_t = (s_s - s_r)/t_s \\ t_{DOY},1...366 \end{cases} \quad (6)$$

Radiation reduction is probably the most important concern when growing a crop under an agrivoltaic system. Our software calculates radiation reduction at different time resolutions: instantaneous, daily, and seasonal. In this work, it was computed during maize growth (April to September), at pixel level, $\boldsymbol{Q_{R,pn}}$(%), for multiannual simulation (1976–2014) as:

$$\boldsymbol{Q_{R,p_n}} = \left(1 - \frac{\sum_{d=doy_e}^{d=doy_h} (\boldsymbol{R_{g,p_n}})_d}{\sum_{d=doy_e}^{d=doy_h} (\boldsymbol{R_{g,0}})_d}\right) 100 \quad (7)$$

where $\boldsymbol{R_{g,0}}$ (kJ m^{-2}) is the daily global radiation in open air, $\boldsymbol{doy_e}$ and $\boldsymbol{doy_h}$ are, respectively, the day of year of crop emergence and harvest.

Radiation reduction values were then classified for each pixel and year at the level of the unit study area (Fig. 5b) attributing each value to a class of a set of ten, each with an interval of 5% radiation reduction: 0–5, 5–10, …, 45–50.

2.4. Estimation of electrical power and Land Equivalent Ratio (LER)

Electricity production from PV panels $Y_{kWh_{sn}}$ (Eq. (8)), was computed for all simulations (4 scenarios on the 39 years) during crop cultivation (April to September), with the same meteorological database used for crop simulation, but with a time step of 1 h. Electricity production was computed per m^2 of PV panel but was then converted and presented per m^2 of cultivated soil using the ratio ν_{sn} of PV panels per cultivated area (Table 2). A constant value of efficiency $\eta = 0.14$ was assumed to convert solar radiation $R\beta_h$ intercepted by PV panels to electricity.

$$Y_{kWh,agv_{sn}} = \nu_{sn}\eta \sum_{h=1}^{Nh} R\beta_h \quad (8)$$

Hourly values $R\beta_h$ were computed following procedures described by Maleki et al. [39] with:

$$R\beta_h = Rd\beta_h + Rb\beta_h + Rr_h \quad (9)$$

where $Rd\beta_h$,$Rb\beta_h$ and Rr_h are respectively the diffuse, beam and reflected radiation.

The Land Equivalent Ratio (LER), developed to estimate the productivity of land when a mixture of crops is used [40–41], was proposed by Dupraz et al. [21] as indicator of land productivity under agrivoltaic systems. In our study LER, calculated as in Eq. (10), is used to compare *Agrovoltaico* scenarios to maize monocrop obtained under full light.

$$LER_{sn} = \frac{Y_{crop,agv_{sn}}}{Y_{crop,FL}} + \frac{Y_{kWh,agv_{sn}}}{Y_{kWh,PV}} \quad (10)$$

where $Y_{crop,agv_{sn}}$ is the total dry matter or grain yield (kg m^{-2}) obtained in one of the *Agrovoltaico* scenarios which is compared to $Y_{crop,FL}$, (kg m^{-2}) obtained in full light conditions as monocrop. Similarly, $Y_{kWh,agv_{sn}}$ and $Y_{kWh,PV}$ (kWh·m^{-2}) are the electrical yields obtained respectively under an *Agrovoltaico* scenario and a reference PV plant (ground mounted) that maximize electricity production. The reference grown mounted PV in our study, has the same characteristics of *Agrovoltaico* 'rel 2', operating in sun-track with a panel density $\nu_{PV} = 0.36$ (Table 1 and Fig. 1c), which is the PV plant configuration that maximises electricity production. We decided to adopt this configuration because a panel densities higher than 0.36, would result in an excessive self-shading and consequent loss of efficiency (Rem Tech, personal communication). In order to compare the energy productivity of solar panels and crop, the potential electrical yield from maize was also estimated. This calculation was performed assuming the maize biomass

Table 2
LER of four Agrovoltaico systems estimated with simulations. Mean values over the period 1976 – 2014.

Configuration	Sun track	Ratio: total panels surface/ soil surface	Electricity from PV (kWh·m^{-2})	Electricity from biogas [¥] (kWh·m^{-2})	Grain yield (g m^{-2})	Biomass yield (g m^{-2})	LER based on grain yield	LER based on biomass yield	Ratio agrovoltaico energy/conventional
Monosystem PV-sun track	Yes	0.36	64.04	–	–		–	–	
Full Light				2.41	705	2080	–	–	
Agrovoltaico ST1	Yes	0.13	17.42	2.43	735	2091	1.31	1.28	0.60
Agrovoltaico F1	No	0.13	11.73	2.53	793	2178	1.31	1.23	0.43
Agrovoltaico ST2	Yes	0.36	64.04	2.47	743	2131	2.05	2.02	2.00
Agrovoltaico F2	No	0.36	43.43	2.55	781	2202	1.79	1.74	1.39

[¥] Electrical energy computed assuming biogas transformation according to Agostini et al. [42].

was processed in an anaerobic digestion plant producing biogas which is fed to an engine coupled to the electrical generator. Parameters are given by Agostini et al. [42].

2.5. GECROS model component

The crop model GECROS (for v1.0, see [30]) predicts crop biomass and yield as affected by climatic factors (radiation, temperature, wind speed, and partial vapour pressure) and available amount of soil water and nitrogen. The model represents crop responses of individual physiological processes to environmental variables, thereby embodying mechanisms that drive crop dynamics and generate emergent feedback features. This model has been independently implemented and validated for simulation the productivity of several crops (including maize) (e.g. Wu et al. [43]), as well as for ecosystems simulation, e.g. MXL-GECROS [44], DANUBIA [45]. For the latter application it was concluded that GECROS has proved its suitability for large-scale research where site-specific calibration is unfeasible and standard parameter values must be used.

The core of GECROS is to model photosynthesis and transpiration. For our simulation study, GECROS v3.0 [46] was used. In this version, leaf photosynthesis rate (A) was calculated from the analytical algorithms that are based on the biochemical model described by Farquhar et al. [47] for C_3-photosynthesis, and its equivalent for C_4-photosynthesis [48], coupled with a phenomenological diffusional conductance model (for overview, see [49] and references therein). The analytical cubic polynomials (see [49]) simultaneously solve stomatal conductance (g_s), internal [CO_2] level, and leaf photosynthesis rate (A) for a given temperature. The obtained g_s was used in the Penman-Monteith equation [50] for surface energy balance to model leaf transpiration and leaf temperature as affected by factors such as radiation, vapour pressure, and [CO_2]. Leaf temperature was then used for re-calculating leaf photosynthesis and transpiration. The effect of leaf nitrogen content on photosynthesis, g_s and transpiration is reflected by the effect of leaf nitrogen on leaf parameters of the photosynthesis model.

Spatial extension from leaf to canopy photosynthesis and transpiration was established using the sun/shade model [51] where the canopy is divided into sunlight and shaded fractions and each fraction is modelled separately with a single-layer leaf model. To represent the realism of agrivoltaic conditions where, at a given time of a day, a specific portion of soil (pixel) may receive only diffuse light, photosynthesis is computed without sun/shaded distinctions and the whole canopy is considered in the shade. The photosynthesis and evapotranspiration subroutines were fed with the radiation levels obtained with the earlier described model, and instantaneous values of photosynthesis and evapotranspiration were computed for 24 time-points during the day-light period of each diurnal cycle. Daily totals of photosynthesis and transpiration were computed from the 24 time points of instantaneous values.

These approaches for spatial and temporal extensions apply to the case in the absence of water stress. In the presence of water stress (i.e. water availability does not satisfy the requirement for potential transpiration), diurnal course of available water is assumed to follow that of radiation, and the available water at each diurnal moment is partitioned between sunlit and shaded leaves according to the relative share of their potential transpiration to obtain their instantaneous actual transpiration. The actual transpiration is transformed into the actual level of g_s using the Penman-Monteith equation, and the actual g_s was then used as input to an analytical quadratic model to estimate the instantaneous actual photosynthesis of the leaves. Again, daily totals were computed from the 24 time points of instantaneous values.

In addition to photosynthesis and transpiration, crop phenology, leaf area development, soil evaporation, nitrogen uptake, partitioning of carbon and nitrogen assimilates among growing organs, accumulation and remobilisation of carbon and nitrogen reserves, and leaf and root senescence are all modelled, in either direct or an indirect response to environmental factors like radiation, temperature, vapour pressure, [CO_2], and soil nitrogen and water availability [30].

2.6. Crop simulation

The simulation work was divided into three main steps.

(1) To compute shading and radiation at a resolution of 0.12 m for the *Agrovoltaico* scenarios described in Table 4.

Listed scenarios differ for panel management: static (**F**) with a fixed tilt angle of 30°, or sun-track (**ST**) and 2 panel configurations, differing for the number of panels mounted on the secondary axis. A non-shaded, full light (**FL**) simulation scenario was also added to have a base-line situation.

These scenarios were chosen to analyze, on maize yield, the shading effect of 2 actual *Agrovoltaico* configurations installed in Italy (Fig. 1), both equipped with the sun-tracking system but with configuration differing for total panels area (single or double). Simulations with static panels were also introduced as this is the most common configuration for photovoltaic panels.

The agronomic input set for scenarios 1–5 (Table 4) were: rainfed crop and 20 g m^{-2} of total N.

Two additional scenarios 6–7 (Table 4) with full irrigation (no water limitations) were added using panel configuration ST2 and full light.

(2) To prepare input files for **GECROS** at a wider resolution: from 0.12 m to 0.48 m with the calculation of a mean radiation value obtained from 16-high resolution pixels. GECROS was run at reduced resolution to simulate the whole area in a reasonable computation time and without affecting significantly results. Dynamic calculation of shaded areas was carried out at the highest possible resolution (0.12 m) in SciLab, while higher resolutions would have required the use of external libraries such as gdal-libraries [GDL - GNU Data Language http://gnudatalanguage.sourceforge.net/] that allow very complex 3D calculations. In this phase of the project we preferred to favor the simplicity of our calculation platform. Simulations with GECROS were run at a lower resolution (0.48 m) to represent a soil surface

Table 3
GECROS model: values of crop growth for maize and soil parameters.

Crop parameters		Unit	Value	Reference
C3C4		–	−1	Gecros switch variable for C4 crops
TBD	Base temperature for phenology	°C	8	[30]
TOD	Optimal temperature for phenology	°C	29	[30]
TCD	Ceiling temperature for phenology	°C	42	[30]
LWIDTH	Leaf width	m	0.05	[30]
CDMHT	Stem dry weight per unit of plant height.	$g\,m^{-2}\,m^{-1}$	570	Pioneer, http://www.agronomico.com
RDMX	Maximum rooting depth	cm	145	Pioneer, http://www.agronomico.com
SLNMIN	Minimum or base SLN (specific leaf nitrogen content) for photosynthesis	$g\,N\,m^{-2}$	0.4	[67]
LNCI	Initial critical shoot N concentration	$g\,N\,g^{-1}$	0.05	[67]
RNCMIN	Min N concentration in root	$g\,N\,g^{-1}$	0.005	[67]
STEMNC	Min N concentration in stem	$g\,N\,g^{-1}$	0.008	[67]
SLA0	Specific leaf area constant	$m^2\,m^{-2}$	0.025	[52]
EAJMAX	Energy of activation of Jmax.	$J\,mol^{-1}$	70,890	[30]
PMEH	Fraction of sigmoid curve inflection in entire plant height growth period	–	0.85	Gecros default value
YGV	Growth efficiency of vegetative organs	$g\,C\,g^{-1}C$	0.81	[30]
CFV	Carbon fraction in vegetative organs	$g\,C\,g^{-1}$	0.48	Gecros default value
FFAT	Fraction of fat in storage organs	$g\,fat\,g^{-1}$	0.047	Gecros default value
FLIG	Fraction of lignin in storage organs	$g\,lignin\,g^{-1}$	0.12	Gecros default value
FOAC	Fraction of organic acids in storage organs	$g\,organic\,acid\,g^{-1}$	0.02	Gecros default value
FMIN	Fraction of minerals in storage organs	$g\,mineral\,g^{-1}$	0.01	Gecros default value
FPRO	Fraction of proteins in storage organs	$g\,protein\,g^{-1}$	0.1	Gecros default value
FCAR	Fraction of carbohydrates in storage organs	$g\,carbohydrate\,g^{-1}$	0.72	Gecros default value
SEEDW	Weight of a single seed	$g\,seed^{-1}$	0.32	Pioneer, http://www.agronomico.com
SPSP	DS for start of photoperiod-sensitive phase	–	0.2	[30]
EPSP	DS for end of photoperiod-sensitive phase	–	0.7	[30]
MTDR	Minimum thermal days for reproductive phase (seed filling)	day	36	Pioneer, http://www.agronomico.com
MTDV	Minimum thermal days for vegetative growth phase	day	54	Pioneer, http://www.agronomico.com
HTMX	Max plant height	m	2.7	Pioneer, http://www.agronomico.com
XJN	Leaf photosinthesis. Slope of linear relationshipe between JMAX and leaf nitrogen.	$\mu mol\,e^-\,s^{-1}\,g^{-1}\,N$	120	Gecros default value
XVN	Leaf photosinthesis. Slope of linear relationshipe between VCMC and leaf nitrogen	$\mu mol\,CO_2\,s^{-1}\,g^{-1}\,N$	60	Gecros default value
Soil parameters				
CLAY	Percentage of clay in the soil	%	29	(Italy, regional services)[a]
WCMIN	Minimum soil water content	$m^3\,m^{-3}$	0.166	Italy, regional services
HUMR	Decomposition rate costant	yr^{-1}	0.02	Defaul value [30]
BIOR	Decomposition rate costant	yr^{-1}	0.66	Defaul value [30]
RN	Residual nitrate N in the soil	$g\,N\,m^{-2}$	1.5	–
RA	Residual ammonium N in the soil	$g\,N\,m^{-2}$	3	–
BHC	Initial value for microbial biomass + humified organic matter in the soil	$g\,C\,m^{-2}$	4400	Italy, regional services
TOC	Total organic C in the soil	$g\,C\,m^{-2}$	7193	Italy, regional services

[a] ARPAV - Emilia Romagna region, Geological, Seismic and Soil Survey

Table 4
Simulated scenarios and conditions.

N.	Scenario	Code	Simulation years	Simulation settings	
				Water	Total N input
1	Release 1 - sun track	**ST1**	From 1976 to 2014	Rainfed	$20\,g\,m^{-2}$
2	Release 1 - static	**F1**			
3	Release 2 - sun track	**ST2**			
4	Release 2 - static	**F2**			
5	Full light	**FL**			
6	Release 2 - sun track	**ST2 (NL)**	1987, 2004	No limited	$20\,g\,m^{-2}$
7	Full light	**FL (NL)**			

comparable to that occupied by a maize plant and row distances, which are comparable to the resolution adopted by Colaizzi et al. [52].

(3) To run GECROS over the study area (144 m^2 or 625 pixels).

Steps 1, 2 and 3 were repeated over a period of 39 years (1976–2014) using the input weather of Castelvetro, Piacenza, Italy (latitude: 45.07°, longitude: 9.93°, elevation: 36 m) where an actual *Agrovoltaico* system was built (Fig. 1). The simulated crop was maize with a simple management scheme: planting date 15 April, rainfed, and nitrogen fertilizer of 13 and 7 $g\,N\,m^{-2}$ applied respectively at planting and 50 days after planting. Crop and soil parameters are listed in Table 3.

Considering all years, scenarios and pixels more than 10^5 runs of GECROS were carried out.

3. Results

We divided the crop cycle into the three main development phases: lag phase (the period between emergence and start of exponential growth ("Em-LagE"); crop establishment (the period including exponential growth to grain-set ("LagE-Gra"); and crop maturity (the period including grain filling and crop senescence ("Gra-Mat").

Rainfall was highly variable (Fig. 4), especially in the lag phase (Em-LagE), which was approximately between the second week of May and mid-July. The average rainfall during the whole crop cycle was 290 mm. The driest years were 1987, 2003 and 2006, when 153 mm, 77 mm and 64 mm of rainfall was recorded, respectively. The highest rainfall (489 mm) was recorded in 1982.

Mean air temperature tended to increase with the simulation years (Fig. 3). As a consequence, the duration of the development phases decreased, especially for Em-LagE and LagE-Mat.

Mean global radiation was 18.7, 22.8 and 20.6 $MJ\,m^{-2}\,d^{-1}$ respectively in the three development phases. In 1987, during the Em-LagE phase, the highest global radiation registered during the simulation period, associated with limited rainfall (153 mm), created a particularly stressful condition for plant growth (Fig. 4). On the contrary, 2004 registered relatively low global radiation (mean value

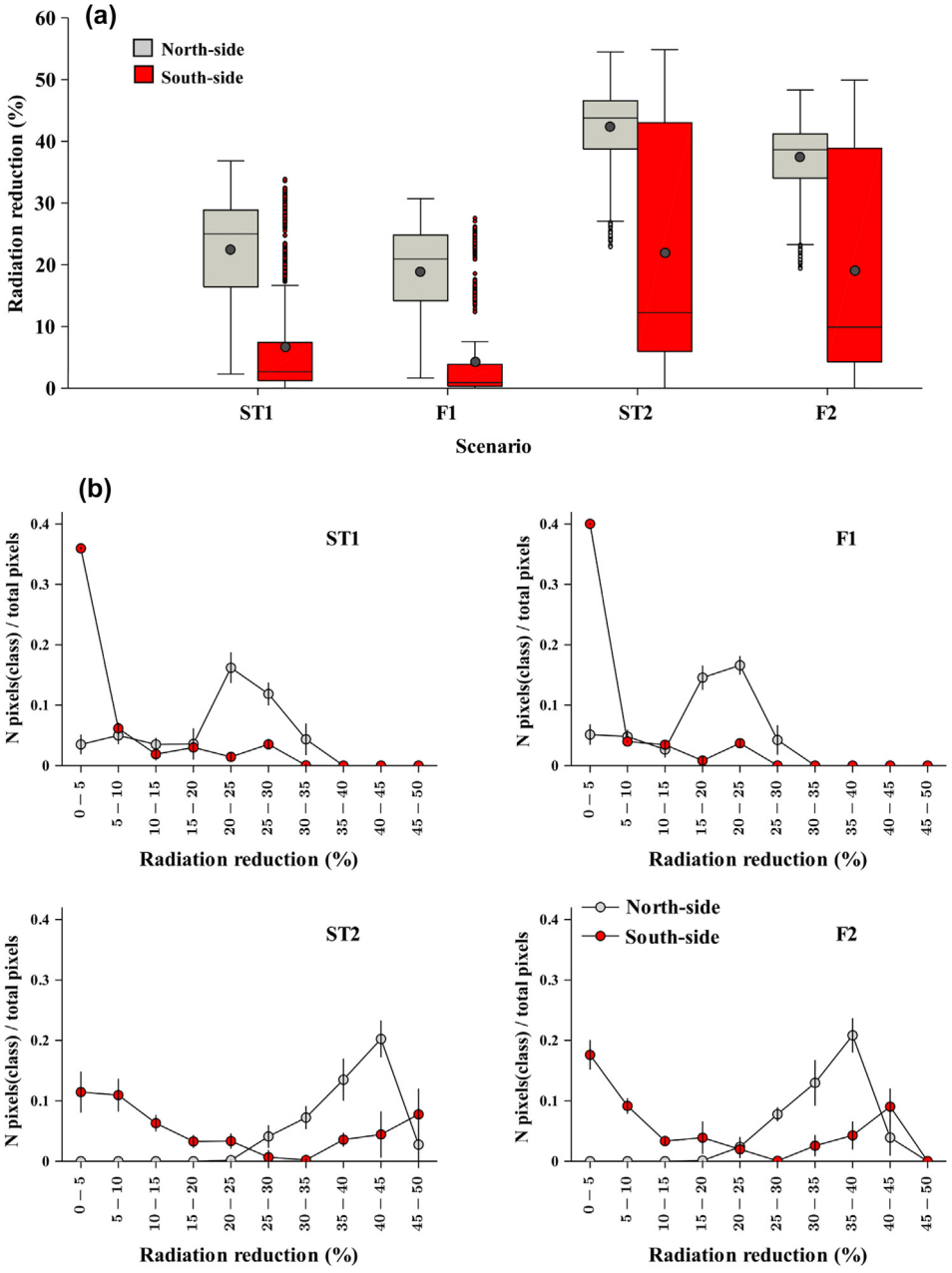

Fig. 6. (a) Radiation reduction in the four scenario and pixel position. (b) Frequencies distribution of radiation reduction computed in four Agrovoltaico scenarios and pixel position in the study area (● North-side) and below (● South-side) of the main rotation axis, see Fig. 4b. Frequencies were computed as ratio between the number of pixels of a radiation reduction class and total pixels. Circles are mean values computed with data of seasonal radiation reduction of 39 years, equation.7, (period 1976–2014) and the vertical bars are the standard errors.

14.3 MJ m^{-2} d^{-1}) and lower than average rainfall over the whole crop cycle (172 mm), that was however quite abundant in the Em-LagE phase.

Reduction of global radiation under the *Agrovoltaico* system was more affected by solar panel (SP) area (single panels, scenario 1 and double panel, scenario 2) than by panel management (static, F and sun-track, ST). During the simulation period, mean radiation reduction was 14.6%, 12.1%, 31.8%, and 27.9% respectively in ST1, F1, ST2 and F2 (see Table 4 for codes and scenarios description). Considering the whole study area (12 m x 12 m), the range of variability of simulated radiation reduction was higher with double panels than with single panels and with sun track than with static panels (Fig. 6). In particular, by dividing the study area into two parts, it was noted that the area at the south of the rotation axis had the highest frequency of pixels with a low reduction of global radiation, while the opposite was true for the area at the north (Fig. 6), indicating that within the study area radiation reduction was highest in the north part. Year by year variability, indicated by the standard error of frequencies of radiation reduction, was relatively limited (Fig. 7).

Radiation reduction affected simulated mean soil temperature, evapotranspiration (ET) and water balance (Fig. 7). In all years mean soil temperature was lower under *Agrovoltaico* than in full light (FL) conditions (Fig. 7a), with a mean difference of 1 °C. Similarly for cumulated ET (Fig. 7b), values under *Agrovoltaico* were lower than in FL, except in very dry years. Mean ET over the entire period was 442 mm and 477 mm respectively in *Agrovoltaico* and FL. In Fig. 7c seasonal water balance is represented for all simulated years. Seasonal water balance was −10.3 mm and −46 mm respectively under *Agrovoltaico* and FL.

3.1. Grain yield

Mean grain yield (DM, g m^{-2}) over the whole simulation period for all four *Agrovoltaico* scenarios (F1, F2, ST1, ST2) and FL are presented in Fig. 7a. Surprisingly the lowest average grain yield was obtained under FL conditions. It is also interesting to note that the highest year to year

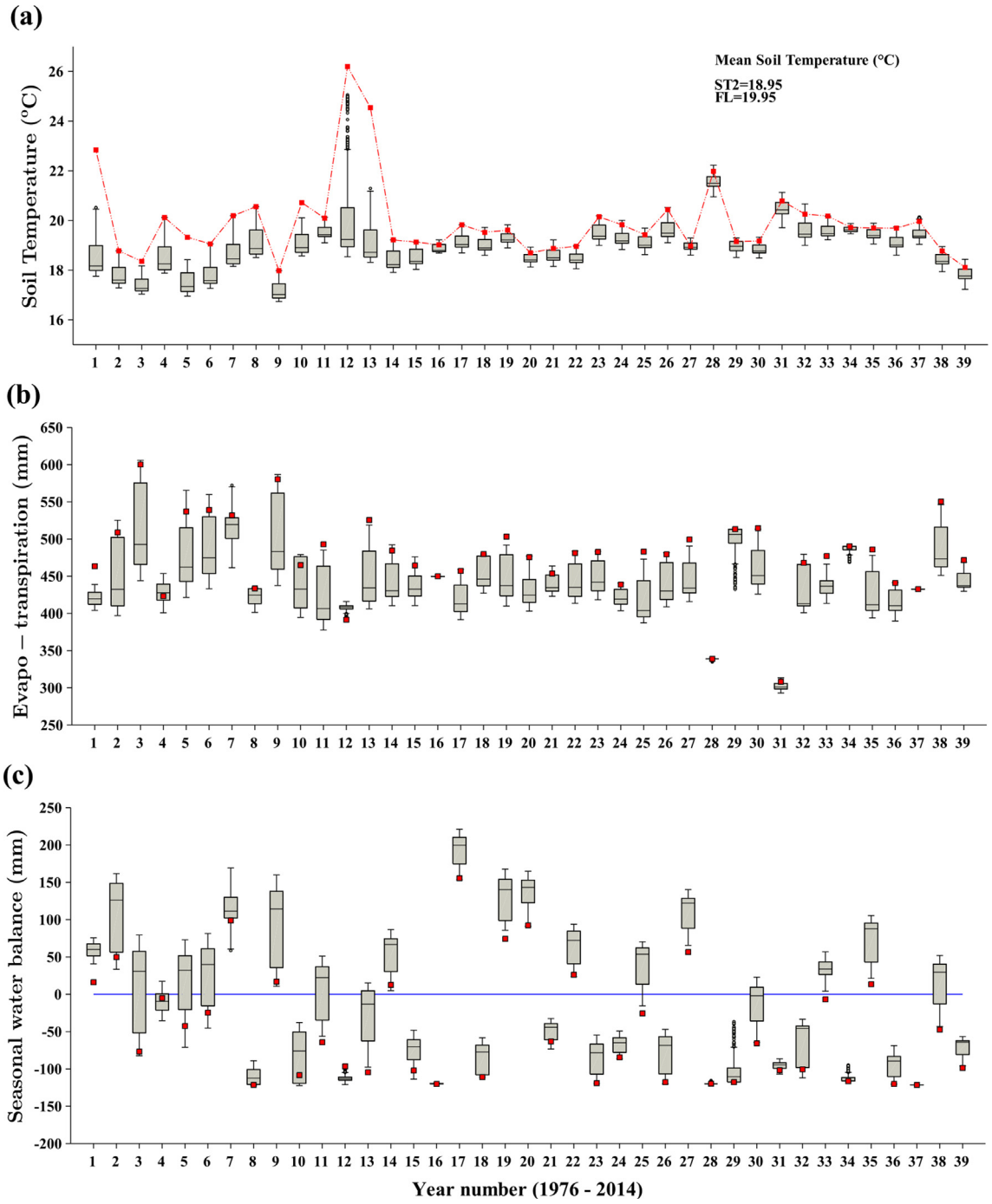

Fig. 7. (a) Mean values of simulated soil Temperature (°C) in rooted layer, (b) seasonal evap-transpiration (mm) and (c) seasonal water balance. The box plots represent the data variability within the Agrovoltaico scenario ST2 for each simulation year. The red squares indicate simulated values in FL. Water balance (WB) was estimated with: WB = Iswc + R-ET, where Iswc is the water content at emergence (field capacity), R is rainfall between emergence and harvest and ET is the seasonal crop evpotranspiration computed by Gecros model. (For interpretation of the references to colour in this figure legend, the reader is referred to the web version of this article.)

variability was also obtained under FL conditions, with the lowest and the highest yield observed in 1987 and 2004, when 182.2 g m^{-2} and 1196.6 g m^{-2} were obtained, respectively. In the same two years, the lowest and highest yields were also observed under *Agrovoltaico* scenarios, which indicates that in 1987 and 2004 extreme weather patterns produced very large yield variations that are worth considering as paradigmatic situations for interpreting and comparing the model output obtained under *Agrovoltaico* and FL (see Section 3.2).

Comparing *Agrovoltaico* scenarios it emerged that under static panels maize reached a higher average yield than under sun tracking panels. Solar panel area (single vs double panels) affected grain yield only in the case of sun-tracking, as scenario ST2 produced a bit less than ST1 with a mean difference of 8.3 g m^{-2} (1.2%). Differences of grain yield for static panels were also limited: 11.7 m^{-2} (1.4%). Conversely, for static panels the double panel (F2) ensured the highest simulated mean productivity under *Agrovoltaico*.

Representation of data from all scenarios in the form of probability exceedance (Fig. 8b) shows that the highest yields could be achieved under FL but, the probability associated to a yield higher than 1000 g m^{-2} was rather low (less than 20%). The same was true in

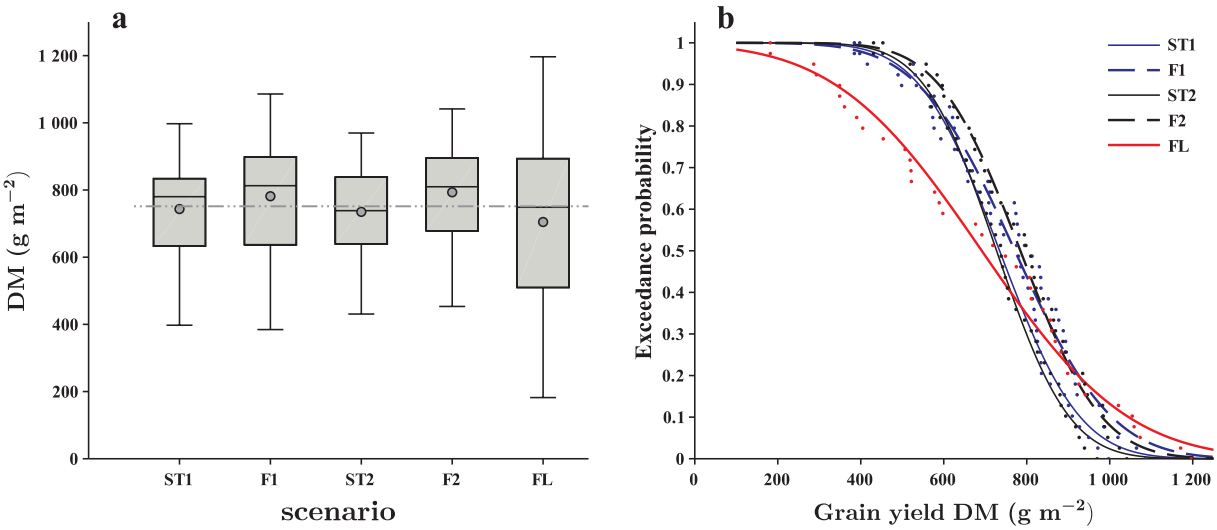

Fig. 8. (a) Mean grain yields (DM, g m^{-2}) for the whole simulated period (1976–2014) obtained in rainfed conditions with four Agrovoltaico scenarios and in full light (FL). The dotted gray line represents the general mean (all years all scenarios). The horizontal gray continuous line and the gray dots represent respectively the median and the mean value. (b) Exceedance probability of grain yield computed for the five scenarios using the whole data-set of the simulated period (1976–2014).

Agrovoltaico scenarios (less than 10%), however, the probability to exceed average yield (~800 g m^{-2}) was ~75%, while it was only 51% in the case of FL. Within *Agrovoltaico* scenarios, the highest probability to achieve average yields for rainfed maize was observed for scenarios F1 and F2 (Fig. 8b).

To exemplify how grain yield varies under *Agrovoltaico* due to micrometeorological conditions, results of grain yield simulations per year relative to scenario ST2 are shown in Fig. 8. Each boxplot describes the yield variability within the study area for each year of the simulation period. Overall, mean grain yield for ST2 and FL (Fig. 9) was respectively 735 g m^{-2} and 704.7 g m^{-2}. Within-year variability was surprisingly high, which indicates that yield simulations run on each pixel of the study area give very variable results and in several years differences between the most and least productive pixels exceeded 1000 g m^{-2}. Yield differences among years, driven by variable weather conditions, were also remarkable. The lowest and highest average yield for FL were 198 g m^{-2} and 1197 g m^{-2} respectively and for ST2 were 202 g m^{-2}and 1476 g m^{-2} respectively, which underlines, again, that year-to-year yield variations were greater under FL than under *Agrovoltaico*.

3.2. Effect of mean radiation reduction on grain yield

The relation between radiation reduction and grain yield obtained under scenarios ST2 and FL in 1987 and 2004, is presented in Fig. 10a for simulations run with full irrigation (to prevent drought stress), and in Fig. 10b for simulations run in rainfed conditions.

Under FL and full irrigation average grain yield was 1719 and 1415 g m^{-2} (Fig. 10a), in 1987 and 2004 respectively. Considering that water was not limiting, the higher yield obtained in 1987 than in 2004 was due to the higher radiation. For *Agrovoltaico* with full irrigation, radiation reduction (at any level) always affected grain yield, with reductions ranging from 1% to 35%. Under mild shading (20–35% radiation reduction) grain yields under *Agrovoltaico* were quite close to those obtained in FL. From a thorough analysis of the spatial distribution of yield data within the study area it emerged that a clear distinction between pixels positioned to the north and south of the rotation axis existed. In both years, yield was higher in the north pixels (Fig. 10a) than in the south pixels, but differences were most obvious in 1987.

In rainfed conditions, the contrasting radiation intensity between the two years produced a large difference in grain yield. In 1987, a very dry year, grain yield was always higher under *Agrovoltaico* than under

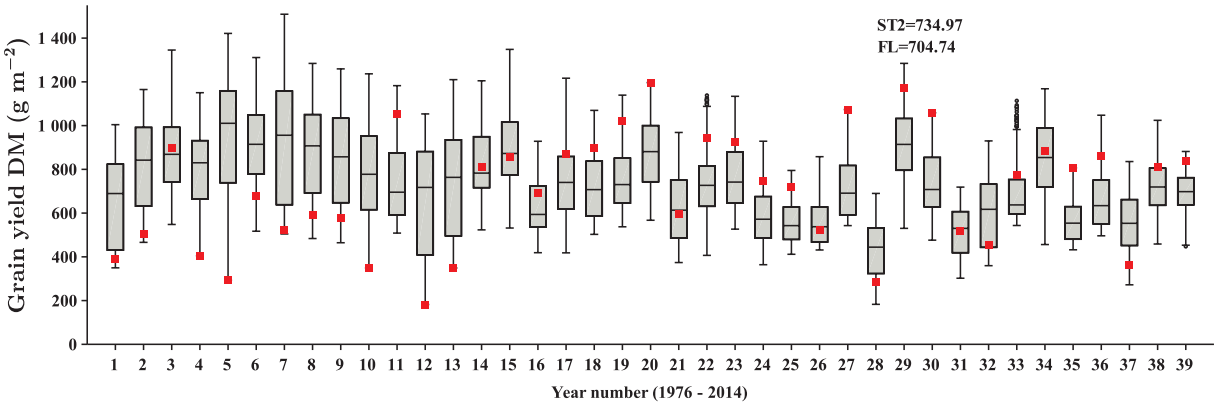

Fig. 9. Annual grain yields (DM, g m^{-2}) in the period (1976–2014) for Agrovoltaico scenario ST2 (rainfed). The box plots represent the data variability within each simulation year. The boxes indicate the 1st and 3rd quartiles of the distribution, the bold line is the median, the bars are the maximum and minimum, the points represent the outliers and gray circles indicate outlying values, far more than 1.5 the interquartile distance. The red squares (■) indicate grain yield simulated in open air conditions. (For interpretation of the references to colour in this figure legend, the reader is referred to the web version of this article.)

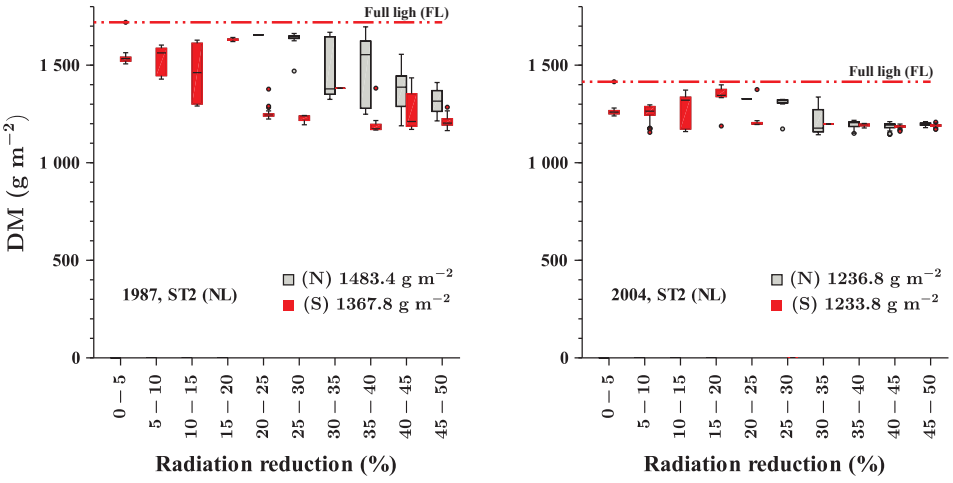

Fig. 10a. Relation between seasonal radiation reduction (%) and simulated annual grain yield in two contrasting years, (1987 and 2004) for scenarios ST2 in no limiting conditions (NL) of water. Data are given for the areas occupied by pixels located above (■ North-side) and below (■ South-side) of the main rotation axis, see Fig. 4b. The dotted, horizontal line represents simulated grain yield obtained in full light (FL).

FL and this difference increased proportionally to radiation reduction up to a value of 40%.

In 2004, when rainfall satisfied crop water demand, grain yield was on average higher in FL than under *Agrovoltaico* scenarios. The highest grain yield under *Agrovoltaico*, matching those obtained under FL, was found for scenarios ST2 and F2 in the pixels with moderate radiation reduction (20 and 25%) while a higher radiation reduction resulted in a progressive yield decrease.

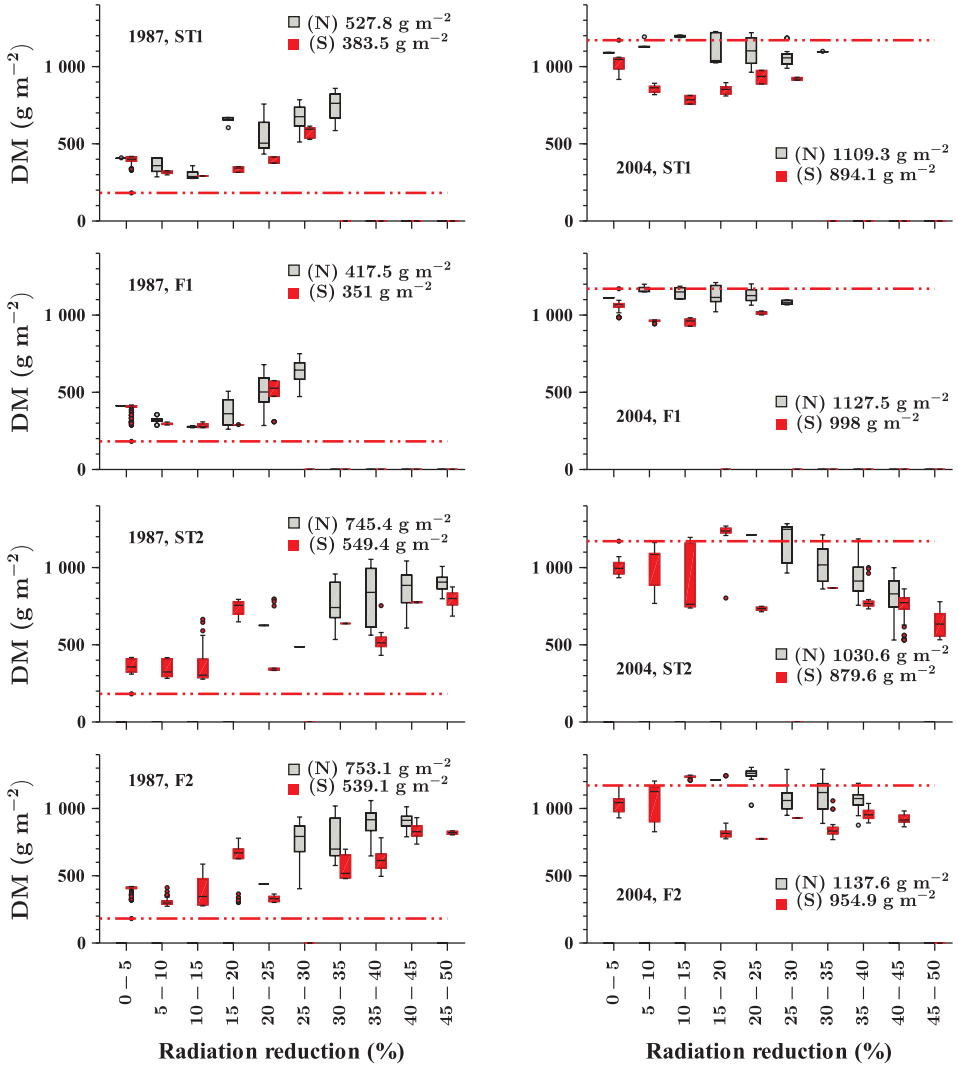

Fig. 10b. Relation between seasonal radiation reduction (%) and simulated annual grain yield in two contrasting years, (1987 and 2004) in four Agrovoltaico scenarios in rainfed conditions. The dotted, horizontal line represents simulated grain yield obtained in full light (FL). Values on the right of (N) and (S) are the mean yields (g m^{-2}) in the North side and South side of the study area.

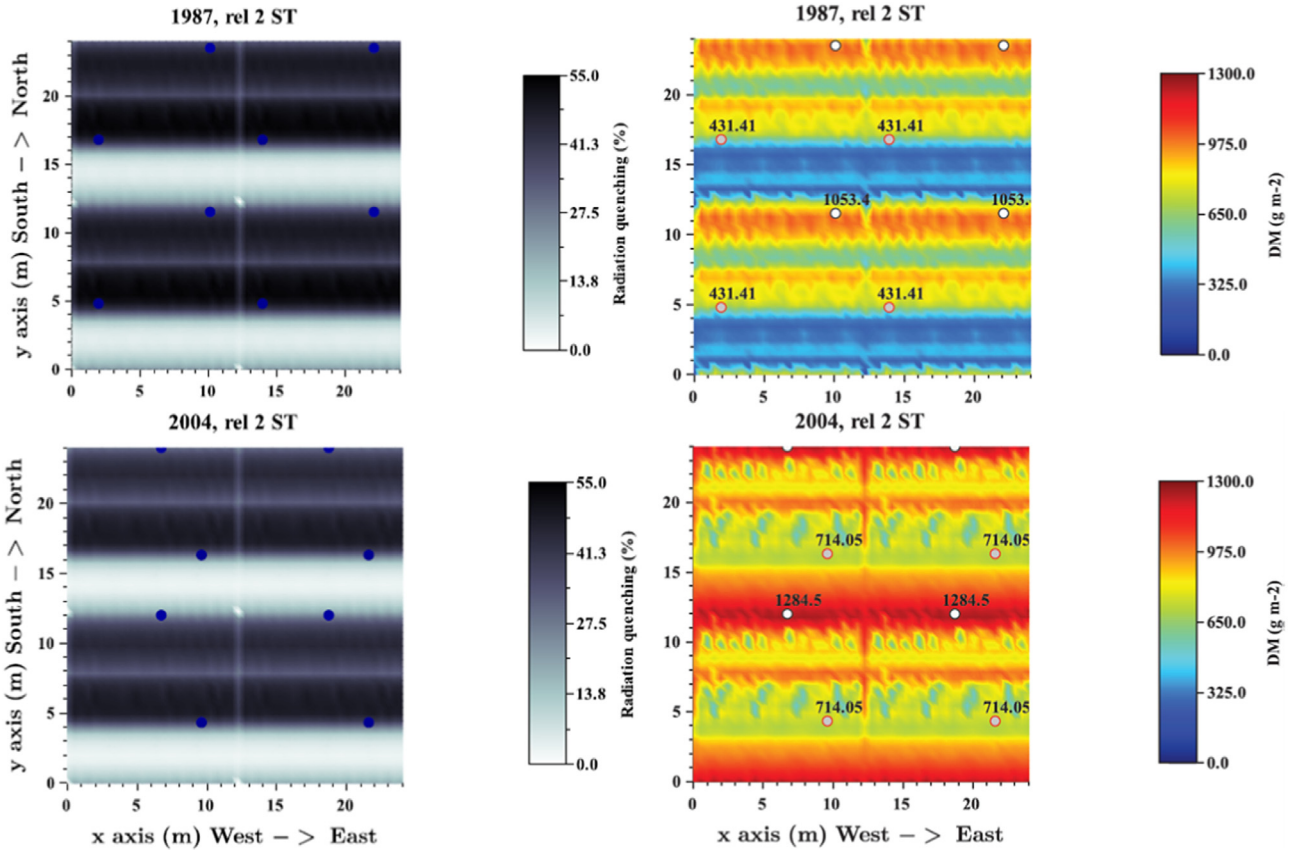

Fig. 11. Maps of seasonal radiation reduction to open air condition (%) and simulated grain yield (g m^{-2}) in two contrasting years, drought and rainy (1987 and 2004) under an Agrovoltaico system, scenario 'ST2'. Each map was obtained by juxtaposition of four sub-maps and, each sub-map, represents a single 'study area' (Fig. 4b) of 625 simulation plots (pixels) of 0.48 m width. The gray and white dots represent respectively the low yield (LY) and high yield (HY) plots belonging to the same radiation reduction class in the respective year.

As already observed in non-limiting conditions as well as in rainfed conditions, north pixel performed better than south pixel and the difference was more evident in 1987, the driest year, than in 2004 (Fig. 9b).

Comparing maps of radiation reduction with those of simulated grain yield for the two contrasting years, 1987 and 2004 (Fig. 11), it appears that the highest yields in 2004 were obtained in pixels where radiation was relatively high, while in 1987, the highest yields were achieved in pixels with low radiation. In Fig. 11 (right) gray and white dots represent pixels that achieved respectively the lowest and the highest yield within the same range of annual radiation reduction that was 40–45% in 1987 and 25–30% in 2004. As previously noted, 'low yield' pixels (gray) lie in the south side and 'high yield' pixels lie in the north side of the main rotation axis. A physiological explanation of how the north and south side generate low and high yielding pixels is provided in the supporting material.

3.3. Biomass yield and energy production

In the area where the *Agrovoltaico* system is installed, a significant proportion of maize crops are destined to biogas production and numerous ground mounted PV plants exist. This creates a case for comparing the global land productivity of the *Agrovoltaico* systems, which combines the production of maize to that of PV energy, to the common option of cultivating maize for biogas and producing electric energy from ground mounted PV systems on separate fields.

During the simulation years (1976–2014), annual global horizontal radiation ranged from 1200 to 1659 kWh·m^{-2} with an average value of 1398 kWh·m^{-2}. Global horizontal radiation during the maize growing period (approximately five months, from mid-April to early September), represented nearly half of the annual value (45.5%) with an average value of 636 kWh·m^{-2}. Mean electricity outputs (Fig. 12) calculated along the simulation period, followed a trend parallel to that of the global seasonal irradiation. In particular, during the period of maize cultivation and for the four Agrovoltaico scenarios (ST1, F1, ST2 and F2), average electricity outputs from PV were highest with sun tracking and at the highest panel density (Table 2). It should be noted that as reference "ground mounted PV system" it was considered a sun tracking system identical to "*Agrovoltaico* 2ST", as this is the PV configuration that maximizes electric energy production (data not shown).

As a measure of global land productivity, the Land Equivalent Ratio (LER) was calculated considering the electric energy produced, per unit surface, by photovoltaics panels and the grain and biomass yield obtained with maize cultivated under *Agrovoltaico* scenarios, or under FL. LER value is always above 1, which indicates that any Agrovoltaico scenario is more advantageous than the separate production of maize for biogas and electric energy from ground mounted PV systems, and LER increased with panel density and it was higher with sun tracking than with static panels (Table 2). Similar results were obtained using whole maize biomass, instead of seed yield. Considering the fix factor 1.16 kWh (kg biomass)$^{-1}$ to convert maize biomass into electric energy from biogas, it was possible to calculate the overall electric energy production of a unit surface of Agrovoltaico (the total electricity from PV from biogas), and to compare it with electricity produced from PV and biogas separately. The energy production per unit surface was lowest under *Agrovoltaico* in both scenarios having low panel density, while the opposite was found for high density *Agrovoltaico* panels (Table 2).

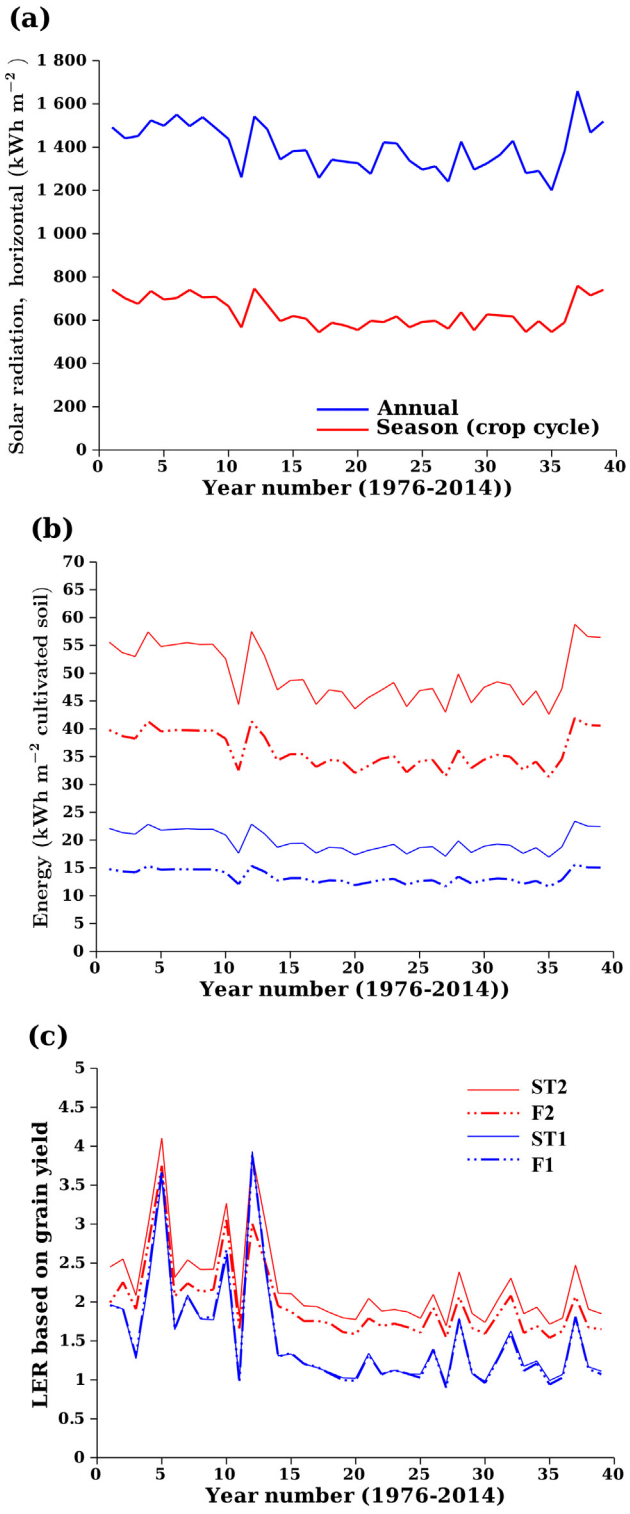

Fig. 12. Mean annual values of horizontal global irradiation (kWh·m^{-2}) (a). Simulated seasonal electrical energy output (kWh·m^{-2}) of four Agrovoltaico scenarios. The outputs were estimated between maize crop emergence and harvest (b). Land equivalent ratio (LER) based on grain yield, estimated for the Agrovoltaico system (c).

4. Discussion

In this work a novel modeling platform, realized to study and optimize the integration of photovoltaic systems with field crop production, is first described and then used to run a scenario analysis in which the yield of maize is simulated under different configurations of an agrivoltaic system (*Agrovoltaico*) installed in the north of Italy (Emila Romagna Region, PC). The actual *Agrovoltaico* system has a relatively low panel area/land area ratio (0.135) and a full sun tracking system is implemented to maximize radiation interception and energy production. To broaden the impact of our modelling study, the effect of shading on the yield of a maize crop was simulated considering: the actual *Agrovoltaico* system configuration (ST1); an additional scenario in which the panel area was increased (ST2 panel area/land area ratio of 0.36) and, for both scenarios, the options with static panels (F1 and F2). Alternative scenarios, while providing a wider spectrum of conditions for testing crop response to shading, represent potential optimizations of the actual system to increase energy production per unit area (high panel density), to balance production of energy and biomass or to reduce construction costs (with static systems).

The climatic data set used for the simulations provided a wide variability of weather conditions, in line with what is expected in the region [53–54] and adequate to assess the impact of the major weather variables on maize yield grown under different *Agrovoltaico* solutions. Our modelling platform has specific Scilab functions for agrivoltaic conditions to simulate shading, and diffuse and direct radiation of our multi-annual data set on small portions of soil (pixels). This enabled the model to (i) capture the rapidly changing conditions of an agrivoltaic system with a high spatial and temporal resolutions, and (ii) implement a database on shaded and non-shaded portions at ground level. The discrimination between sunlit and shaded soil surface components may not be feasible or even meaningful for energy balance calculated at the field or larger scale, for example, mapping evapotranspiration (ET) using satellite reflectance or land surface temperature measurements [19,55–56]. However, at small spatial scales, as those adopted in this study (i.e., crop row scale), and time steps shorter than 24 h, it is both practical and desirable to consider the large variation in energy balance calculated for sunlit and shaded surfaces [57–58]. Some important practical applications of small scale energy balance models include those that seek to separate the evaporation (E) and transpiration (T) components of ET as proposed by Colaizzi et al. [52,59–60] as the GECROS model does.

The simulation of an agrivoltaic cultivation system requires a crop model able to capture the multiple feedback processes triggered by a fluctuating radiation regime (and its consequences on microclimate). In this context we considered the use of GECROS very appropriate. In fact, the coupling of photosynthesis and transpiration, implemented in GECROS, allows a dynamic response to external stresses through the calculation of the leaf energy balance. This feature is particularly relevant, when simulating a crop grown in an agrivoltaic system, because temporal radiation patterns are simulated at a high time resolution (24 times day^{-1}). The influence of environmental conditions on the biochemical reactions of photosynthesis are consequently well modelled. In addition, estimation of the energy balance at soil level, which is computed by the soil sub-model, benefits from the information on sun/shaded portions for accurate soil evaporation [15,30]. Given the exploratory approach of this study we also assumed the absence of site specific calibration non-relevant. Similar consideration was made by Lenz-Wiedemann et al. [45] using GECROS and obtaining acceptable results for maize simulation (among other crops) without calibration.

In agrivoltaic systems radiation reduction plays a pivotal role as it affects the microclimate under solar panel [25] and excessive shading may compromise the economic feasibility of the crop [23,61] In our simulated experiment average radiation reduction, among the four scenarios, ranged from 12.1% (F1) to 31.8% (ST2) which is lower than values reported by Dinesh and Pearce [23], and much lower than those reported by Dupraz et al. [21], where was found a seasonal radiation reduction of 28.7% and 56.5%, for two agrivoltaic configurations. These differences are partly the consequence of the mounted-height of the panels, that was 4 m in the system described by Dupraz et al. [21] and 4.85 in the *Agrovoltaico*, and partly the consequence of panel

density (panel area/land area ratio), that was lower in the *Agrovoltaico* scenarios (0.135 and 0.36) than in the PV system described by Dupraz et al. [21] (0.285 or 0.59).

A limitation of our computation system was the absence of a micrometeorology subroutine to compute air temperature, wind speed and relative moisture profiles under the Agrovoltaico system (both in the shaded or sunlit areas). Therefore, the same values for micrometeorological parameters calculated under FL were adopted for Agrovoltaico. We assumed this limitation negligible also considering previous research [25] showing that mean daily air temperature, VPD, and wind speed were not significantly affected by PVP compared to full sun conditions. Marrou et al. [25] showed also showed that soil temperature was more affected than air temperature by shading.

Although the calculation of the soil surface and leaf temperatures in GECROS are subject to limitations (they are computed on the basis of the energy balance equations indicated by Penman-Monteith, 1973) we assumed that mean values of the simulations might be useful to interpret the observed phenomena. The average seasonal differences of soil temperature (Fig. 7a) could be explained with the diverse energy load (radiation) reaching the different pixels. The soil temperature differences between FL and *Agrovoltaico* simulated by GECROS are similar to those reported by Marrou et al. [25] which ranged from −0.5 °C to −2.3 °C between shaded and non-shaded soil portions in agrivoltaic experiments involving winter wheat and vegetables. According to Marrou et al. [25] and Colaizzi et al. [52] the differences of ET between shaded parts and FL, as a consequence of the different level of radiation reaching the ground and the crop, are significant, while differences of air temperature, relative humidity and wind speed are small. The differences of evaporation and transpiration between FL and *Agrovoltaico* highlight that fluctuating shading under *Agrovoltaico* improves the use of water, mainly due to reduced soil evaporation (Fig. A1). During maize growing season, on the average of the simulation years, mean evaporation saving under *Agrovoltaico* was 46 mm. Water saving in rainfed conditions can have a significant difference on crop yield. In fact, especially in the years when rainfall was limited in the first phase of crop cycle (e.g. 1987, 1988), the transpiration in FL was very low, proving a clear situation of stress and stomata closure (Fig. A1). It is interesting to note that, despite receiving less radiation than FL, crops grown under Agrovoltaico have a mean transpiration slightly higher than crops grown in FL, over the entire simulation period (Fig. A1). This is probably the consequence of the higher water available under Agrovoltaico than in FL conditions, due to the lower water evaporation, and it is evident that GECROS reacts dynamically to soil water availability adjusting crop transpiration with stomatal closure/opening.

The accuracy with which the model calculates the radiation available under PV panels is crucial to simulate crop production effectively, as it is generally considered that yield limitation under PV panels can be substantial [23]. In the case of maize it is reported that shading limits biomass production by affecting all yield components [62–64], as maize is a C_4 crop, whose photosynthesis increases greatly with increasing light levels. Our simulations are in general agreement with this conclusion under non-limiting conditions (i.e. Fig. 10a), but our results show that water limitations are crucial in the evaluation of shading on crop performance (or yield). Data from long period simulation under rainfed conditions (i.e. Fig. 7, scenario ST2) showed that shading exerted a positive effect on crop growth, mitigating the stress caused by high radiation levels (Fig. 4), particularly when water was limiting. This mitigation is important throughout the whole growing period and in particular during the first part of the crop cycle, when it prevents stunted growth.

As expected, the highest yields (e.g. 1000 g m^{-2}) were obtained under FL conditions, but with a probability lower than 20% (Fig. 8a). Surprisingly, under rainfed conditions, average maize yield was higher under *Agrovoltaico* scenarios than under FL. Furthermore, year to year variation of mean yield was lower under *Agrovoltaico* than under FL (Fig. 9). In fact, in *Agrovoltaico* the coefficient of variation (CV%) of grain yield was 19.3, 22.3, 17.8 and 18.4, for the four scenarios while it was 37.9 in FL. This result highlights that the shading of *Agrovoltaico* has a potential effect of yield stabilization.

The advantage of maize cultivated under *Agrovoltaico* scenarios was evident when water was limited. The favorable effect of shading by solar panels in water limited conditions was already discussed by Marrou et al. [22,25] showing the potential of agrivoltaic systems to mitigate the effects of direct radiation, reducing soil evaporation and increasing water saving.

The *Agrovoltaico* system in its actual configuration (ST1), and to a greater extent in the scenarios presented in this work, provides a very effective strategy to maximize land productivity, especially when electric energy is targeted. Land Equivalent Ratio (LER) calculated for all the *Agrovoltaico* scenarios largely exceeded the value 1, threshold above which the “intercropping” (in our case, PV panels + maize) is more advantageous than the separate production of maize and electric energy from ground mounted PV systems. This result on maize confirms and reinforces what was predicted by Dupraz et al. [21] and successively confirmed by the study described by Valle et al. [27] who obtained high LER (> 1.5) cultivating lettuce under ST systems. In our simulations unprecedented values of LER, above 2 and up to 3, were found under scenario ST2. In this case electric energy from *Agrovoltaico* and ground mounted PV systems was identical, which guarantees that LER has a minimum value of 1, while maize yield was on average similar under *Agrovoltaico* and FL (therefore LER = 2) and, when water was limiting, maize yield was higher under *Agrovoltaico* than FL (therefore LER > 2).

If land productivity is assessed only considering electric energy production, the scene is dominated by PV, whose electric energy production ranges from 11.7 kWh·m^{-2} (scenario F1) to 64.0 kWh·m^{-2} (scenario ST2) while average electric energy from maize biomass when converted to biogas ranges from 2.41 kWh·m^{-2} to 2.55 kWh·m^{-2} [24].

The option of having biogas maize produced under *Agrovoltaico* is more favorable than the option of separate ground mounted PV and dedicated maize for biogas, when using scenarios ST2 or F2 (Table 2).

These results highlight the potential of our simulation platform to study the performance of an agrivoltaic system or to optimize land use for renewable electricity production. An example could be the optimization of electricity production in the province of Piacenza, where the actual *Agrovoltaico* plants are installed. In the province of Piacenza in 2016 the “ground mounted” PV represented 40% of the total 177 MW of PV installed. Given that “ground mounted” PV is 40% of all installed PV and each MW of installed PV occupies 1.9 ha (www.gse.it), it is estimated that 134.5 ha of agricultural land are occupied by PV in the province of Piacenza. In the same province, 8.9 MW of biogas are installed and considering that approximately 50% of the biogas is obtained from dedicated bioenergy crops (mainly maize), we can assume that almost 1400 ha of maize are cultivated each year as dedicated bioenergy crop. From this it can be assumed that 36.44 GWh are produced from biogas maize, while “ground mounted” PV in 2016 produced 75.4 GWh (www.gse.it). The PV panels of an *Agrovoltaico* scenario ST2, under which a crop of maize produces 21.3 t ha^{-1} (average yield of maize under ST2 in this study), on average each year produce 88.41 kWh·m^{-2}. In this example, 1 ha of *Agrovoltaico* ST2 would therefore produce 0.9088 GWh (0.0247 GWh from biogas and 0.8841 GWh from PV) and as a consequence 123 ha of *Agrovoltaico* would be sufficient to produce the same electricity otherwise obtained from the 1534 ha actually used in the province of Piacenza. Of course, this large advantage in land saving is mainly driven by the low energy production of biogas maize per unit surface; the higher electricity yield (kWh_{el} per m^2) of Agrovoltaico’s sun tracking PV panels, than that of the static PV panels of conventional ground mounted PV plants, only plays a minor role. However, from a land-use perspective, it is relevant to note that under conventional ground mounted PV plants crop cultivation is impossible, while, in an Agrovoltaico system, fertile agricultural land is not “grabbed” to sustain renewable energy production [65].

5. Conclusions

An innovative platform was designed and implemented to run simulations aimed at optimizing agrivoltaic systems (North Italy, Emila Romagna Region, PC), where the production of electrical energy is combined to that of arable crops. A long-term simulation, which compared the yield of maize under Agrovoltaico to that of maize in the open field, highlighted that while yield under Agrovoltaico is slightly lower when water is non-limiting, it is higher in conditions of drought stress. In addition, average rainfed maize yield was higher and more stable under Agrivoltaico than in full light conditions. This indicates that agrivoltaic systems, supporting crop yield, clean energy production and water saving, can play a significant role at the energy-food-water nexus [66].

Our modelling platform, implementing the state-of-art crop model GECROS, is a useful tool that can be employed both for predicting the performance of a large number of species and genotypes under specific agrivoltaics conditions, and for optimizing the design and management of the PV infrastructure (e.g. dynamic control of PV panel tilt).

Economic and environmental analysis should be carried out to provide a complete sustainability assessment of the *Agrovoltaico* system, so as to determine which configuration of the *Agrovoltaico* (i.e. specific PV infrastructure design and cropping system) can represent a valuable option to diversify farm income. In this study, data from a long period simulation were used to assess land productivity under Agrovoltaico and to compare it with current land-based renewable energy systems: it is concluded that agrivoltaic systems are very effective in maximizing land productivity, particularly if they are compared to actual renewable energy scenarios in which “ground mounted” PV panels and monocultures of maize for biogas production are supported.

Acknowledgments

The authors would like to thank Ing. Alessandro Reboldi of REM TEC S.r.l. for providing data and information on the Agrovoltaico system and REM TEC S.r.l. for funding part of the activities related to the development of the software platform. The authors thank Dr Francesca O'Kane for linguistic revision.

Appendix A. Supplementary material

Supplementary data associated with this article can be found, in the online version, at http://dx.doi.org/10.1016/j.apenergy.2018.03.081.

References

[1] Dincer I. Renewable energy and sustainable development a crucial review. Renew Sustain Energy Rev 2000;4:157–75. http://dx.doi.org/10.1016/S1364-0321(99)00011-8.
[2] Rajagopal D, Sexton S, Roland-Holst D, Zilberman D. Challenge of biofuel: filling the tank without emptying the stomach? Environ Res Lett 2007;2(4):1–9 < http://iopscience.iop.org/article/10.1088/1748-9326/2/4/044004 > .
[3] REN21. Renewables 2017 global status report, Paris: REN21 Secretariat. ISBN 978-3-9818107-6-9. < http://www.ren21.net/wp-content/uploads/2017/06/17-8399_GSR_2017_Full_Report_0621_Opt.pdf > .
[4] Nonhebel S. Renewable energy and food supply: will there be enough land? Renew Sustain Energy Rev 2005;9(2):191–201. http://dx.doi.org/10.1016/j.rser.2004.02.003.
[5] Rathmann RG, Szklo A, Schaeffer R. Land use competition for production of food and liquid biofuels: an analysis of the arguments in the current debate. Renew Energy 2007;35(1):14–22. http://dx.doi.org/10.1016/j.renene.2009.02.025.
[6] Zanon B, Verones S. Climate change, urban energy and planning practices: Italian experiences of innovation in land management tools. Land Use Policy 2013;32:343–55. http://dx.doi.org/10.1016/j.landusepol.2012.11.009.
[7] Sacchelli S, Garegnani G, Geri F, Grilli G, Paletto A, Zambelli P, et al. Trade-off between photovoltaic systems installation and agricultural practices on arable lands: an environmental and socio-economic impact analysis for Italy. Land Use Policy 2016;56:90–6 < http://agris.fao.org/agris-search/search.do?recordID=US201700099320 > .
[8] Calvert K, Mabee W. More solar farms or more bioenergy crops? Mapping and assessing potential land-use conflicts among renewable energy technologies in eastern Ontario, Canada. Appl Geogr 2015;56:209–21. http://dx.doi.org/10.1016/j.apgeog.2014.11.028.
[9] Fthenakis V, Kim CK. Land use and electricity generation: a life-cycle analysis. Renew Sustain Energy Rev 2009;13:1465–74. http://dx.doi.org/10.1016/j.rser.2008.09.017.
[10] Scognamiglio A. ‘Photovoltaic landscapes’: design and assessment. A critical review for a new transdisciplinary design vision. Renew Sustain Energy Rev 2016;55:629–61. http://dx.doi.org/10.1016/j.rser.2015.10.072.
[11] Xue J. Photovoltaic agriculture - new opportunity for photovoltaic applications in China. Renew Sustain Energy Rev 2017;73:1–9. http://dx.doi.org/10.1016/j.rser.2017.01.098.
[12] Bennamoun L. Integration of photovoltaic cells in solar drying systems. Drying Technol 2013;31(11):1284–96. http://dx.doi.org/10.1080/07373937.2013.788510.
[13] Han C, Liu J, Liang H, Guo X, Li L. An innovative integrated system utilizing solar energy as power for the treatment of decentralized wastewater. J Environ Sci 2013;25(2):274–9. http://dx.doi.org/10.1016/S1001-0742(12)60034-5.
[14] Campana PE, Leduc KM, Olsson A, Zhang J, Liu J, Kraxner F, et al. Suitable and optimal locations for implementing photovoltaic water pumping systems for grassland irrigation in China. Appl Energy 2017;185:1879–89.
[15] Mondino EB, Fabrizio E, Chiabrando R. Site selection of large ground-mounted photovoltaic plants: a GIS decision support system and an application to Italy. Int J Green Energy 2015;12(5):515–25. http://dx.doi.org/10.1080/15435075.2013.858047.
[16] Cuce E, Harjunowibowo D, Cuce PM. Renewable and sustainable energy saving strategies for greenhouse systems: a comprehensive review. Renew Sustain Energy Rev 2016;64:34–59. http://dx.doi.org/10.1016/j.rser.2016.05.077.
[17] Sgroi F, Tudisca S, Di Trapani AM, Testa R, Squatrito R. Efficacy and efficiency of Italian energy policy: the case of PV systems in greenhouse farms. Energies 2014;7:3985–4001. http://dx.doi.org/10.3390/en7063985.
[18] Cossu M, Murgia L, Ledda L, Deligios PA, Sirigu A, Chessa F, et al. Solar radiation distribution inside a greenhouse with south-oriented photovoltaic roofs and effects on crop productivity. Appl Energy 2014;133:89–100. http://dx.doi.org/10.1016/j.apenergy.2014.07.070.
[19] Li C, Wang H, Miao H, Ye B. The economic and social performance of integrated photovoltaic and agricultural greenhouses systems: case study in China. Appl Energy 2017;190:204–12. http://dx.doi.org/10.1016/j.apenergy.2016.12.121.
[20] Goetzberger A, Zastrow A. On the coexistence of solar-energy conversion and plant cultivation. Int J Sol Energy 1982;1:55–69. http://dx.doi.org/10.1080/01425918208909875.
[21] Dupraz C, Marrou H, Talbot G, Dufour L, Nogier A, Ferard Y. Combining solar photovoltaic panels and food crops for optimising land use: towards new agrivoltaic schemes. Renew Energy 2011;36(10):2725–32. http://dx.doi.org/10.1016/j.renene.2011.03.005.
[22] Marrou H, Wery J, Dufour L, Dupraz C. Productivity and radiation use efficiency of lettuces grown in the partial shade of photovoltaic panels. Eur J Agron 2012;44:54–66. http://dx.doi.org/10.1016/j.eja.2012.08.003.
[23] Dinesh H, Pearce JM. The potential of agrivoltaic systems. Renew Sustain Energy Rev 2016;54:299–308 < http://linkinghub.elsevier.com/retrieve/pii/S136403211501103X > .
[24] Dupraz C, Talbot G, Marrou H, Wery J, Roux S, Liagre F, et al. To mix or not to mix: evidences for the unexpected high productivity of new complex agrivoltaic and agroforestry systems 2011. In: Proceedings of the 5th world congress of conservation agriculture: resilient food systems for a changing world. < http://aciar.gov.au/files/node/13992/to_mix_or_not_to_mix_evidences_for_the_unexpected_19701.pdf > .
[25] Marrou H, Guilioni L, Dufour L, Dupraz C, Wery J. Microclimate under agrivoltaic systems: is crop growth rate affected in the partial shade of solar panels? Agric For Meteorol 2013;177:117–32. http://dx.doi.org/10.1016/j.agrformet.2013.
[26] Majudmar D, Pasqualetti MJ. Dual use of agricultural land: introducing ‘agri-voltaics’ in Phoenix Metropolitan Statistical Area, USA. Lands Urban Plan 2018;170:150–68. http://dx.doi.org/10.1016/j.landurbplan.2017.10.011.
[27] Valle B, Simonneau T, Sourd F, Pechier P, Hamard P, Frisson T, et al. Increasing the total productivity of a land by combining mobile photovoltaic panels and food crops. Appl Energy 2017;206:1495–507. http://dx.doi.org/10.1016/j.apenergy.2017.09.113.
[28] rem TEC Monticelli; 2017. < http://www.remtec.energy/en/agrovoltaico/monticellidongina-plant/ > .
[29] rem TEC 2017 Castelvetro < http://www.remtec.energy/en/agrovoltaico/castelvetro-plant/ > .
[30] Yin X, Van Laar H. Crop systems dynamics: an ecophysiological simulation model for genotype-by-environment interactions. Wageningen Academic Pub.; 2005. ISBN: 13 978-90-76998-55-8.
[31] Scilab Enterprises and Consortium Scilab. Digiteo. Scilab: Free and OpenSource software for numerical computation (OS, Version 5.4.1); 2012 [Software] < http://www.scilab.org > .
[32] Collares-Pereira M, Rab A. The average distribution of solar radiation-correlations between diffuse and hemispherical and between daily and hourly insolation values. Sol Energy 1979;22:155–64. http://dx.doi.org/10.1016/0038-092X(79)90100-2.
[33] Wanxiang Y, Zhengrong L, Tongbin X, Yuan L, Xiaobin L. New decomposition models to estimate hourly global solar radiation from the daily value. Sol Energy 2015;120:87–99. http://dx.doi.org/10.1016/j.solener.2015.05.038.
[34] Al-Rawahi NZ, Zurigat YH, Al-Azri NA. Prediction of hourly solar radiation on horizontal and inclined surfaces for Muscat/Oman. J Eng Res 2011;8:19–31 < https://journals.squ.edu.om/index.php/tjer/article/view/98/104 > .

[35] Ephrath JE, Goudriaan J, Marani A. A modelling diurnal patterns of air temperature, radiation wind speed and relative humidity by equations from daily characteristics. Agric Syst 1996;51(4):377–93. http://dx.doi.org/10.1016/0308-521X(95)00068-G.
[36] Reda I, Afshin A. Solar position algorithm for solar radiation applications. Natioanl Renewable Energy Laboratory (NREL); Technical report NREL/TP-560-3402; 2008 < http://www.nrel.gov/docs/fy08osti/34302.pdf > .
[37] Quaschning V. Hanitsch, R. Shade calculations in photovoltaic systems. ISES Solar World Conference - Harare/Zimbabwe - September 11-15, 1995.
[38] CelesteLab Ver 3.0.0 - Space mechanism for Scilab (c) Centre National d Etudes Spatiales (CNES-DCT/SB, 2003, France) < https://atoms.scilab.org/toolboxes/celestlab > .
[39] Maleki SAM, Hizam H, Gomes C. Estimation of hourly, daily and monthly global solar radiation on inclined surfaces: models re-visited. Energies 2017;10(134). https://dx.doi.org/10.3390/en10010134.
[40] Riley J. A general-form of the land equivalent ratio. Exp Agric 1984;20:19–29. http://dx.doi.org/10.1017/S0014479700017555.
[41] Smith RG, Atwood LW, Warren DW. Increased productivity of a cover crop mixture is not associated with enhanced agroecosystem services. PLOS ONE 2014;9(5):e97351. http://dx.doi.org/10.1371/journal.pone.0097351.
[42] Agostini A, Battini F, Giuntoli J, Tabaglio V, Padella M, Baxter D, et al. Environmentally sustainable biogas? The key role of manure co-digestion with energy crops. Energies 2015;8(6):5234–526. http://dx.doi.org/10.3390/en8065234.
[43] Wu W, Ma YP, E YH, Sun LL, Jing YS. Adaptability evaluation of GECROS simulating summer maize growth in the Yellow-Huaihe-Haihe Rivers. Acta Agronomica Sinica 2015;41(01):123–35.
[44] Combe MJ, De Arellano VG, Ouwrsloot HG, Jacobs CMJ, Peters W. Two perspectives on the coupled carbon, water and energy exchange in the planetary boundary layer. Biogeosciences 2015;12:103–23. http://dx.doi.org/10.5194/bg-12-103-2015.
[45] Lenz-Wiedemann VIS, Klar CW, Schneider K. Development and test of a crop growth model for application within a Global Change decision support system. Ecol Model 2010;221:314–29. http://dx.doi.org/10.1016/j.ecolmodel.2009.10.014.
[46] Yin X. Improving ecophysiological simulation models to predict the impact of elevated atmospheric CO_2 concentration on crop productivity. Ann Bot 2013;112:465–75. http://dx.doi.org/10.1093/aob/mct016.
[47] Farquhar GD, von Caemmerer S, Berry JA. A biochemical model of photosynthetic CO_2 assimilation in leaves of C_3 species. Planta 1980;149:78–90. http://dx.doi.org/10.1007/BF00386231.
[48] von Caemmerer S, Furbank RT. Modeling of C_4 photosynthesis. In: Sage RF, Monson R, editors. C_4 plant biology. San Diego (CA, USA): Academic Press; 1999. p. 169–207. < http://www.esalq.usp.br/lepse/imgs/conteudo_thumb/C4-Plant-Biology-by-Rowan-Sage-and-Russell-Monson–1999-.pdf > .
[49] Yin X, Struik PC. C_3 and C_4 photosynthesis models: An overview from the perspective of crop modelling. NJAS Wageningen J Life Sci 2009;57:27–38. http://dx.doi.org/10.1016/j.njas.2009.07.001.
[50] Monteith JL. Principles of environmental physics. London: Edward Arnold; 1973. < http://www.scirp.org/(S(351jmbntvnsjt1aadkposzje))/reference/ReferencesPapers.aspx?ReferenceID=48012 > .
[51] de Pury DGG, Farquhar GD. Simple scaling of photosynthesis from leaves to canopy without the errors of big-leaf models. Plant Cell Environ 1997;20:537–57. http://dx.doi.org/10.1111/j.1365-3040.1997.00094.x.
[52] Colaizzi PD, Evet SR, Agam N, Schwartz RC, Kustas WP. Soil heat flux calculation for sunlit and shaded surfaces under row crops: 1. Model development and sensitivity analysis. Agric For Meteorol 2016;216:115–28. http://dx.doi.org/10.1016/j.agrformet.2015.10.010.
[53] Bocchiola D, Nana E, Soncini A. Impact of climate change scenarios on crop yield and water footprint of maize in the Po valley of Italy. Agric Water Manage 2013;116:50–61. http://dx.doi.org/10.1016/j.agwat.2012.10.009.
[54] Amaducci S, Colauzzi M, Battini F, Fracasso A, Perego A. Effect of irrigation and nitrogen fertilization on the production of biogas from maize and sorghum in a water limited environment. Eur J Agron 2016;76:54–65. http://dx.doi.org/10.1016/j.eja.2016.01.019.
[55] Kalma JD, McVicar TR, McCabe MF. Estimating land surface evaporation: a review of methods using remotely sensed surface temperature data. Surv Geophys 2008;29:421–69. http://dx.doi.org/10.1007/s10712-008-9037-z.
[56] Kustas WP, Anderson MC. Advances in thermal infrared remote sensing for land surface modeling. Agric For Meteorol 2009;149(12):2071–81. http://dx.doi.org/10.1016/j.agrformet.2009.05.016.
[57] Agam N, Kustas WP, Evett SR, Colaizzi PD, Cosh M, McKee LG. Soilheat flux variability influenced by row direction in irrigated cotton. Adv Water Resour 2012;50:20–30. http://dx.doi.org/10.1016/j.advwatres.2012.07.017.
[58] Evett SR, Agam N, Kustas WP, Colaizzi PD, Schwart RC. Soil profile method for soil thermal diffusivity, conductivity, and heat flux: comparison to soil heat flux plates. Adv Water Resour 2012;50:41–54. http://dx.doi.org/10.1016/j.advwatres.2012.04.012.
[59] Colaizzi PD, Agam N, Tolk JA, Evett SR, Howell TA, Gowda PH, et al. Two-source energy balance model to calculate E, T, and ET: comparison of priestley-taylor and penman-monteith formulations and two time scaling methods. Trans ASABE 2014;57(2):479–98http://dx.doi.org/10.13031/trans.59.11215.
[60] Colaizzi PD, Evett SR, Howell TA, Gowda PH, O'Shaughnessy SA, Tolk JA, et al. Two-source energy balance model: Refinements and lysimeter tests in the Southern High Plains. Trans ASABE 2012;55(2):551–62http://dx.doi.org/10.13031/2013.41385.
[61] Castellano S. Photovoltaic greenhouses: evaluation of shading effect and its influence on agricultural performances. J Agric Eng 2014;45(433):168–75 < http://www.agroengineering.org/index.php/jae/article/view/jae.2014.433/pdf_9 > .
[62] Mbewue DMN, Hunter RB. The effect of shade stress on performance of corn silage versus grain. Can J Plant Sci 1986;66:53–60. http://dx.doi.org/10.4141/cjps86-007.
[63] Reed AJ, Singletary V, Schussler JR, Williamson DR, Christy AL. Shading effects on dry matter and nitrogen partitioning, kernel number, and yield of maize. J Exp Bot 2014;65(2):641–53https://dx.doi.org/http://dx.doi.org/10.2135/cropsci1988.0011183X002800050020x.
[64] Pioneer. 2015. Solar radiation and crop needs. < https://www.pioneer.com/CMRoot/Pioneer/US/Non_Searchable/agronomy/cropfocus_pdf/solar-radiation-corn-2015.pdf > .
[65] van der Ploeg JD, Franco JC, Borras Jr. SM. Land concentration and land grabbing inEurope: a preliminary analysis. Can J Dev Stud/Revue canadienne d'études du développement 2015;36(2):147–62. http://dx.doi.org/10.1080/02255189.2015.1027673.
[66] Bazilian M, Rogner H, Howells M, Hermann S, Arent D, Gielen D, et al. Considering the energy, water and food nexus: towards an integrated modelling approach. Energy Policy 2011;39:7896–906. http://dx.doi.org/10.1016/j.enpol.2011.09.039.
[67] Ciampitti IA, Zhang H, Friedemann P, Vyn TJ. Potential physiological frameworks for mid-season field phenotyping of final plant N uptake, N use efficiency and grain yield in maize. Crop Sci 2012;52:2728–42.